ELECTROMAGNETIC INDUCTION FOR IMPROVED TARGET

LOCATION AND SEGREGATION USING SPATIAL POINT

PATTERN ANALYSIS WITH APPLICATIONS TO HISTORIC

BATTLEGROUNDS AND UXO REMEDIATION

A Dissertation

by

CARL JAMES PIERCE, JR

Submitted to the Office of Graduate Studies of
Texas A&M University
in partial fulfillment of the requirements for the degree of

DOCTOR OF PHILOSOPHY

August 2010

Major Subject: Geophysics

ELECTROMAGNETIC INDUCTION FOR IMPROVED TARGET

LOCATION AND SEGREGATION USING SPATIAL POINT

PATTERN ANALYSIS WITH APPLICATIONS TO HISTORIC

BATTLEGROUNDS AND UXO REMEDIATION

A Dissertation

by

CARL JAMES PIERCE, JR

Submitted to the Office of Graduate Studies of
Texas A&M University
in partial fulfillment of the requirements for the degree of

DOCTOR OF PHILOSOPHY

Approved by:

Chair of Committee,	Mark Everett
Committee Members,	D. Bruce Dickson
	Christopher Mathewson
	Hongbin Zhan
Head of Department,	Andreas Kronenberg

August 2010

Major Subject: Geophysics

ABSTRACT

Electromagnetic Induction for Improved Target

Location and Segregation Using Spatial Point

Pattern Analysis with Applications to Historic

Battlegrounds and UXO Remediation. (August 2010)

Carl James Pierce, Jr., B.A. State University of New York at Potsdam;

M.S. Texas A&M University

Chair of Advisory Committee: Dr. Mark Everett

 Remediation of unexploded ordnance (UXO) and prioritization of excavation

procedures for archaeological artifacts using electromagnetic (EM) induction are studied

in this dissertation. Lowering of the false alarm rates that require excavation and artifact

excavation prioritization can reduce the costs associated with unnecessary procedures.

   Data were taken over 5 areas at the San Jacinto Battleground near Houston, Texas,

using an EM-63 metal detection instrument. The areas were selected using the

archaeological concepts of cultural and natural formation processes applied to what is

thought to be areas that were involved in the 1836 Battle of San Jacinto.

   Innovative use of a Statistical Point Pattern Analysis (PPA) is employed to identify

clustering of EM anomalies. The K-function uses point {x,y} data to look for possible

clusters in relation to other points in the data set. The clusters once identified using K-

function will be further examined for classification and prioritization using the Weighted

K-function. The Weighted K-function uses a third variable such as millivolt values or time decay to aid in segregation and prioritization of anomalies present.

Once the anomalies of interest are identified, their locations are determined using the Gi-Statistics Technique. The Gi*-Statistic uses the individual Cartesian{x, y} points as origin locations to establish a range of distances to other cluster points in the data set. The segregation and location of anomalies supplied by this analysis will have several benefits. Prioritization of excavations will narrow down what areas should be excavated first. Anomalies of interest can be located to guide excavation procedures within the areas surveyed.

Knowing what anomalies are of greater importance than others will help to lower false alarm rates for UXO remediation or for archaeological artifact selection. Knowing significant anomaly location will reduce the number of excavations which will subsequently save time and money. The procedures and analyses presented here are an interdisciplinary compilation of geophysics, archaeology and statistical analysis brought together for the first time to examine problems associated with UXO remediation as well as archaeological artifact selection at historic battlegrounds using electromagnetic data.

TABLE OF CONTENTS

LIST OF FIGURES

LIST OF TABLES

1. INTRODUCTION

Electromagnetic Induction (EMI) is a geophysical technique whose principles are broadly similar to those of conventional metal detection. EMI studies on historic battlegrounds provide excellent conditions for studying subsurface metal-bearing targets that have been buried for a substantial length of time. The targets are generally in unknown orientations at varying depths, unknown size and composition. They have been subjected to the rigors of war, soil settling conditions, anthropogenic disturbance, weathering, and corrosion. The consequent in-situ conditions enable us to study these targets in a real world situation and not as an engineered "sand box" investigation.

Detection of buried metal targets has become commonplace and there are many instruments available commercially that are designed specifically for this purpose. These instruments range from hand-held metal detectors that operate mostly in the frequency domain with limited depth-penetration to approximately 30cm, to the advanced research-grade models used by geophysicists that operate in the time domain (e.g EM-63 by Geonics) and frequency domain (e.g. GEM-3 by Geophex) with the ability to probe larger depths up to 5m.

The ability to discriminate a target of interest or a cluster of targets of interest, from clutter is a current gap in the knowledge base that will be addressed in this study. The

_____

This dissertation follows the style of Geophysics.

implications of this research relate directly to unexploded ordnance (UXO) remediation and archaeology. Typically 70 to75% percent of the anomalies excavated on remediation sites (Butler, 2004) are actually not UXO. False alarm rates from non-hazardous items such as UXO fragments, range scrap, and cultural debris account for the rest of the anomalies present. For this reason UXO clean-up costs are expensive. Any improvement in electromagnetic geophysics techniques that can reduce the false alarm rate while preserving the probability of actual UXO detection, will cut the overall cleanup costs significantly

   Through the use of wide area EM-63 assessment and statistical point pattern analysis archaeologists and geophysicists can perform inter-disciplinary study that furthers knowledge in the interfacial region between the two fields. By providing an outdoor laboratory for geophysical data acquisition, the archaeologist may be able to make more accurate historical reconstructions from the spatial distributions of found artifacts. The spatial distributions that are based on cluster analysis performed with statistical point pattern statistical techniques with various weighting factors to aid in anomaly selection. Weighting factors that are considered here are the EM millivolt response and decay time. The fieldwork at San Jacinto Battleground (Figure 1) provided an outdoor laboratory for geophysical data collection. In addition, by precisely locating the positions of historic artifacts at the site. The work has expanded archaeological understanding of the way in which the historic battle at this site unfolded.

Figure 1. Location of San Jacinto Battleground site 10 miles east
of Houston, TX. (Microsoft Streets and Trips 2002)

2. HISTORY

San Jacinto Battleground is located in east Texas ~20 km east of Houston TX. As a direct result of the battle at San Jacinto On April 21, 1836, (Moore, 2004) Texas gained its independence from Mexico. After the massacre at the garrison at The Alamo on March 6th by forces of Mexican general Antonio López de Santa Anna, the Texan commander General Sam Houston, and a small force of ~ 800-900 men, led a surprise attack on the Mexican army near the mouth of the San Jacinto River. With the war cry of "Remember The Alamo!", Houston's smaller army defeated the Mexican force of ~1300 men in less than 20 minutes. Nearly all of Santa Anna's men were either killed or captured in the rout. General Santa Anna, who was among those taken prisoner, signed a treaty that eventually granted Texans their independence and ended the war.

Because the battle began and ended so quickly, little trace of its original location remains. We located subsurface metal artifacts left behind after the battle. By plotting the location and distribution of these artifacts and performing a cluster analysis, archaeologists can constrain the location of the battle and better determine the manner in which it unfolded. A similar combination of geophysical surveying, archaeological excavation and artifact mapping has led to an expanded understanding the Battle of the Little Big Horn in North Dakota (Scott, Fox, Connor and Harmon 1989; Fox and Wood 1993).

3. GEOLOGY AND SOILS

The soil classification on the site is the Nahatche Loam (USDA, 1976) which is part of the Holocene Deweyville Formation. The surface layer is friable, medium acid, dark grayish brown loam~0-12 cm thick. The layer below is ~12-45cm thick that is friable, medium acid, grayish brown loam over firm, moderately alkaline, gray clay loam that has mottles of light gray and brownish yellow. The area is mainly pasture land located on the San Jacinto River annual floodplain of a low relief.

The area around the battle site is subject to perennial inundation and ground subsidence. We can only speculate the subsidence rates for most of the 19th century up to 1893. The majority of the 2.3m subsidence since 1893 occurred (Gabrysch, 1976) during 1943-1973, with the maximum of 1.1m in the period between 1964-1973. The current estimates of subsidence are up to 5cm/yr (Cantrell et. al, 2007) in the Houston-Galveston area. If we project the 5cm/yr rate from 1973 to 2010, the estimate gives us a 4.15m loss in elevation since 1943.

The soil at San Jacinto poses some difficulty with artifact detection using electromagnetic induction techniques. Small clay lenses less than 1m in diameter could produce a cluttering effect. The clay in the soils will tend to produce anomalies that may be interpreted as battle artifacts and raise the false-alarm rate, especially, if they become moist from recent precipitation or other geo-hydrologic processes. The majority of which is caused by the alignment of the electrons on the outer surface of clay particles when they are wetted. There is a mild induced magnetic field effect in that the ends of the clay particles are more negatively charged than the broader sides of flocculated clay

particles. The EM response level of a typical mid-sized(characteristic size, several cm) metal artifact is ~10 millivolts [mV] above the background EM noise level. When several targets are in close proximity there is distortion of the electromagnetic response of each target making locating artifacts difficult or impossible in a clay rich soil.

4. BACKGROUND THEORY

4.1 Geophysical

The law of induction developed by Michael Faraday in 1832 states that "If the magnetic flux [Φ] normal to a plane circuit changes with time, there is an electromotive force generated that is equal in magnitude to the change in flux [$\partial\Phi/\partial t$]. When this occurs, currents will flow in a *closed* circuit such that the magnetic field will align itself in a direction to oppose the change in flux". The direction of the magnetic moment is determined using the "right hand rule" and is equal to *IA* (A/m^2). To visualize this, consider the advance of a right handed corkscrew (Parasnis, 1997) placed at the loop's center when the tips of the handle are turned in the direction of the current in the loop.

A complete motivation of Maxwell's electromagnetic equations is beyond the scope of this dissertation. A pair of damped wave equations, identical in form, that describe the behavior of **B** and **E** field vectors:

$$\nabla^2 \boldsymbol{B} = \mu_0 \sigma \frac{\delta \boldsymbol{B}}{\delta t} + \mu_0 \varepsilon \frac{\delta \boldsymbol{B}}{\delta t^2} \tag{1}$$

$$\nabla^2 \boldsymbol{E} = \mu_0 \sigma \frac{\delta \boldsymbol{E}}{\delta t} + \mu_0 \varepsilon \frac{\delta \boldsymbol{E}}{\delta t^2} \tag{2}$$

$$\text{where} \quad \bar{\nabla}^2 = \frac{\partial^2}{\partial x^2} + \frac{\partial^2}{\partial y^2} + \frac{\partial^2}{\partial z^2} \tag{3}$$

The left side of the equations 1 and 2 describe the variations of **E**, **B** in space. The right sides of the equations show the variations of **E**, **B** with time. The first term on the right side of equation 2 is related to the flow of electricity in a conductor while the second term relates to the displacement current introduced by Maxwell to account for EM wave phenomena. The displacement current is used to describe the extent to which

charges are slightly displaced but not separated from their atoms (Lowrie, 1997) producing an electric polarization. The displacement current is usually negligible (McNeill, 1980) in conductive soils when operating in the typical EM induction frequency range. If we look at equation 1 under these conditions it reduces to:

$$\bar{\nabla}^2 \vec{B} = \mu_0 \sigma \frac{\partial \vec{B}}{\partial t} \qquad (4)$$

To further simplify the discussion we will deal only with EM disturbance in the z-direction where $(\partial/\partial x = \partial/\partial y = 0)$ and $\bar{\nabla}^2 = \partial^2/\partial z^2$. This is the plane wave assumption that has limited application to metal detection, since objects are normally located in the near-field of the transmitter, but aids greatly in the understanding of the essential concepts. In this one-dimensional form equation 1 becomes,

$$\frac{\partial^2 \vec{B}}{\partial z^2} = \mu_0 \sigma \frac{\partial \vec{B}}{\partial t} \qquad (5)$$

If we solve for the components $\vec{B}_x$ or $\vec{B}_y$ for an alternating magnetic field with angular frequency $\omega = 2\pi f$ in a conductor with conductivity σ we get

$$B_{x,y}(z,t) = B_0 e^{-z/d} \cos\left(\omega t - \frac{z}{d}\right) \qquad (6)$$

$$\text{where } d = \sqrt{\frac{2}{\mu_0 \sigma \omega}} \qquad (7)$$

In equation 7, d is known as the "skin depth". At this depth the magnetic field is reduced to e^{-1} or ~ 37% of its value outside the conductor. The skin depth is dependent

on the frequency of the field and the conductivity of the target. Skin depth is an indicator of how quickly the field is attenuated. The magnetic field can penetrate to many times the skin depth[d]. For example, it decays to ~1% at $z = 5d$ and to 0.1% at $z = 7d$.

 Transient field (time domain) methods measure the rate of decay of the secondary field after the primary field is switched off (Sharma, 1997). Frequency domain methods measure the amplitude and phase of the secondary field measured at the receiver. The instrument consists of either a moving coil system in a Slingram or variable-offset (e.g.Geonics EM-47) configuration, or a fixed coil (e.g.Geonics EM-63) central loop configuration.

   Documented studies of transient fields reportedly began in the Soviet Union in the early 1970's, but being in Russian (Fokin, 1971) they are not widely known to scientists in the western hemisphere. Since then there have been several studies (Lee, 1975, Hurley, 1977, Nabighian, 1984 and 1991) on transient pulse responses of conducting spheres and other simple shapes in uncomplicated scenarios. Current studies that have begun to address more complicated shapes and situations (Pierce et al. 2003), (Everett et al. 2005) have shown positive results. The results using multiple orientations of the receiver positions over a target to view the EM response in both secondary horizontal fields of B_x and B_y as well as the common secondary vertical field of B_z have shown sensitivity in imaging the general shape of the target.

4.2 Archaeological

The history of Archaeology is rooted in human curiosity about the past. Ancient cultures wondered about where they had come from and a possible purpose for their existence. Mythological deities were developed by the Ancient Greeks to provide working solutions to these questions. For example, the god Prometheus was claimed to have formed man from clay while the goddess Athena breathed life into him. The brother of Prometheus, Epimetheus, had already endowed gifts such as strength, cunning, wings and fur to the animals he had been tasked to create. Prometheus loved man so much that he stole fire from the gods and presented it to man. Stories such as these provided the answers of questions about creation. Variations on this basic mythology can also be found in the Roman, Egyptian and Aztec civilizations. Although, mythology purports to give answers to the above questions, there is no material evidence to support them. One of the contributions myths makes to archaeology is the impact on the art of these societies. Ancient art has been discovered both by serendipity and in purposeful excavations. Once man began to discover or recognize material evidence of past societies the basis of archaeology began to evolve.

One of the earliest collectors of antiquities (Renfrew and Bahn, 2000) was the last king of Babylon, Nabonidus, who ruled from 555-539 BC. He discovered a old foundation that had been built 2200 years before. He stored and curated this and other artifacts in a kind of museum. During the renaissance (14th-17th centuries), ancient artifacts were unsystematically displayed under the title "natural history". Up to this time archaeology was largely speculative.

In the 18th century the use of scientific methods began with an excavation supervised by the third President of the United States, Thomas Jefferson, on his land in Virginia. In 1784, Jefferson excavated a trench across a burial mound. During the next few years Samuel H. Parsons studied similar mounds in the Ohio country. Parsons corresponded (Parsons, 1786) with Ezra Stiles who relayed this information to Jefferson. These structures were attributed, at the time, to a race of vanished Moundbuilders. Jefferson was careful enough to differentiate layers within the mound. Jefferson also recognized that the lower layers of bone were not as well-preserved as the shallow layers. This indicated to Jefferson that the mounds had been re-used for burial over time. Jefferson formulated a hypothesis that asked the question, "Could the ancestors of the local indigenous people be responsible for the creation of these mounds?" Based on solid evidence within the excavation, he deduced that the possibility did exist. This approach forms the basis of the scientific method used in archaeology today.

The science of geology has long contributed to the development of archaeology. The Scottish geologist James Hutton in his *Theory of the Earth* in 1785 discussed the principles according to which strata are laid down and how their relative age is determined. This concept is used for archaeological excavations and is formally known as the geological "law of superposition". The law of superposition states that the oldest strata are found at the bottom of a formation and strata get progressively younger towards the surface as long as they are not disturbed by later geological processes. Hutton theorized that processes of depositional stratification are currently operating in the oceans, rivers and lakes as they had been throughout time or, simply stated, "the

present is the key to the past." This is called the principle of "uniformitarianism." Charles Lyell further endorsed uniformitarianism in his work *Principles of Geology* (1833) stating that geological conditions in operation now are the same as those that have operated throughout the geological past. Archaeologists have found this principle to be applicable to the past human activities. In many ways current human activities are similar to past activities. An example of this would be the human tendency to build up major communities near a water source. The mass majority of ancient centers of civilization such as Rome, Italy, Alexandria, Egypt and Istanbul, Turkey are built near bodies water. Modern cities of New York, Chicago and Washington D.C are also built near bodies of water.

In 1836, C.J. Thomsen published his guidebook to the National Museum of Copenhagen (Renfrew and Bahn, 2000). Thomsen divided collections of antiquities into three major categories: the Stone Age, Bronze Age and Iron Age. This system of classification was very popular and many Europeam scholars adopted it. Discoveries of chipped stone tools in France during the early 1800's led to ideas that were in conflict with the biblical notion of mankind. Jacques Boucher de Perthes had found some hand-axes in the gravel quarries associated with the Somme River in France. He published his findings in 1841. These tools pre-dated the biblical time frame of human creation and provided evidence of the antiquity of the humankind. Eighteen years later in 1859 Charles Darwin published, *On the Origin of Species*, that described the evolution of plants and animals including man. He called the process "natural selection". The three

major advances; the antiquity of human-kind , the three age system and the theory of evolution form the basic building blocks of modern archaeology.

The use of archaeological techniques can be quite useful to the geophysicist in regards to target (artifact) location and site interpretation. The proper application of formation process in the search for possible archaeological sites and or target areas will increase the possibilities of artifact detection. Archaeologist's are aware of the benefits that geophysics can have upon their research of a site. It should therefore, be a natural progression to apply techniques of archaeology to near-surface geophysical sites at engineering and environmental scales. Formation processes help to make sense of the selection criteria of a specific site and what type of artifacts will be found there.

There are generally two types of formation processes that will be applied to research at San Jacinto Battleground: cultural formation processes and natural formation processes. Cultural formation processes (Rathje and Schiffer, 1982) govern the movements of artifacts from the systemic context to the archaeological context. The systemic record involves artifacts found in locations associated with their intended use. An example of this could be a cooking pot found in the kitchens of the former Pompeii residents. The archaeological record indicates artifacts that have been discarded or moved away from their respective activity area. The best example could be the remnants of a demolished building found at a dump site. The building was moved into archaeological context when pieces of it were transported and discarded.

Cultural formation processes can be divided into four basic categories: (1) re-use (2) deposition, (3) reclamation and (4) disturbance. These categories are linked to what is

known as the *principle of dissociation* (Rathje and Schiffer, 1982) which states: "items found associated with the archaeological record were not necessarily used in the same activity or activity area, and items that were used together are not necessarily found together in archaeological context." If we relate the first part of this principle to the San Jacinto site we could say that a horseshoe found there could be associated with a cavalry horse in the battle or it could be associated with later farming activity. To relate the second part of the principle of dissociation we could say that finding a ramrod of a musket does not necessarily mean that there exists a musket on this site.

To apply the four basic categories of cultural formation process to the Battle of San Jacinto we could say that buttons or pieces of clothing acquired after the battle were re-used on other clothing products or just worn again by the people who found them. Deposition of weapons and other personal belongings happened when the Mexican army was in full retreat of Houston's men towards the area what is now known as Peggy's Lake. Reclamation applies to the return of soldiers and families to gather their dead and personal effects after the battle. What was left over after all of the above could have been moved or trampled by people farming the area or other human related disturbances. There are many possible examples than just the few stated here.

Natural formation processes (Renfrew and Bahn, 2000) are generally concerned with how the environment affects artifact survival in the archaeological record. What can be recovered is dependent upon how it was deposited and the environmental processes that have acted upon it since burial. In general, inorganic materials such as; stone, some metals and fired clays will survive longer in the archaeological record than organic

materials. While this might be the norm, special burial circumstances can preserve organic materials for very long periods. The La Brea tar pits have been providing organic material from creatures trapped millions of years ago. Once the animal was completely coated with the substance it became isolated from the decaying effects of oxygen and preserved quite exquisitely.

Natural formation processes are broken down into four basic categories: (1) nature, (2) duration, (3) effects and (4) scale. Weathering caused by aeolian (wind-generated) processes and moving water are two examples of nature that affect the remains at an archaeological site. Since the San Jacinto site is located on the flood plain moving water would be a process that needs to be taken into consideration. The length of time that an artifact has been buried or exposed will generally affect what is observed in the archaeological record. At San Jacinto the duration of interment is important as the area has been prone to ground subsidence over the past century.   The effects of biological or chemical changes are subtractive since they tend to degrade artifacts. Effects are additive when materials are introduced or attach themselves to artifacts.   At San Jacinto, water generally introduces environmental materials or adds sediments. Scale is sub-divided into three areas: (a) regional, (b) site and (c) artifact. We have considered all three at San Jacinto. San Jacinto Battleground is located in the West Gulf Coastal Plain region, in a sedimentary environment. The site is at the mouth of the San Jacinto River. Fluvial processes before and after the battle will be applicable to our study. The artifacts are yet to be analyzed either in their provenience location (*in-situ*) or by excavation and

curation. Provenience is a more precise burial term that defines "the archaeological find spot" of an artifact (Johnson, 1999).

At this point, several artifacts have been excavated at the site. No analysis is available at this time since the artifacts are still undergoing the curation process. Whether these artifacts are from the actual battle, or not, is currently unknown.

By using the archaeological techniques of formation processes (Schiffer, 1987) geophysicists can possibly increase their chances of detecting artifacts in the subsurface. By studying and applying information gained from formation processes the geophysicist is able to understand how the site has evolved over time. Each site is unique because of the different formation processes that can involve depositional environments, duration of burial and past disturbances either from natural or cultural activities. The unique combination of formation processes a direct affect on the distribution of artifacts and their current state of preservation in the archaeological record. Formation process provides site restraints which can save time and money by limiting the area of coverage needed. Site surveying becomes much more efficient and maximizes the possibility of successful artifact detection. This kind of multi-disciplinary approach provides the geophysicist and archaeologist with a win-win relationship of artifact detection, location, analysis, interpretation and historical documentation. This relationship intrinsically increases the knowledge base of both disciplines and promotes future collaborations in the growing area of Archaeological Geophysics.

4.3 Statistical

Spatial analysis is needed at San Jacinto Battleground because locating anomalies of

interest is a major step in the development of an excavation strategy.   This is one of the

goals of the research undertaken to provide a more economical way to remediate a UXO

site or recover archaeological artifacts. This research required precise location of target

and uses cluster analysis as one method. The statistical technique best suited for

clustering is the K-function (Ripley, 1977). The idea being that the clusters will be at

the same depth in their relative positions within a study area. Then a weighting scheme,

the Weighted K-function (Getis, 1984) is applied to narrow down the locations by use of

a physical property as a 3rd variable. Then precise location is achieved by using the Gi

statistic (Getis and Ord, 1992),

Geostatistics has long been used by geoscientists to evaluate the variation in both

natural and anthropogenic phenomena on and above the land surface. Geostatistics is

more specifically concerned with processes that vary continuosly in space. This applies

to models and techniques developed by (Matheron 1963) to evaluate recoverable

reserves (volume estimation) in the mining industry. For this purpose geostatistics

employs techniques such as variograms and kriging.

Point pattern analysis differs from geostatistical methods (Cressie, 1993) in that point

patterns develop when the important variable to be analyzed is the location of events.

Unlike kriging, (Krige, 1951) spatial point pattern analysis preserves all information

(MacDonald and Small, 2009) about the locations of significant events. Examples of

spatial point patterns include: the locations of trees in a forest, stars in the evening sky,

and the number of nuclei in a microscopic tissue sample. Scientists can use the resulting

patterns from these analyses to make predictions. These analysis techniques show great

promise to our application at San Jacinto Battleground near Houston, TX by establishing

an excavation selection hierarchy.

The statistical "point pattern analysis" (PPA) techniques used for this study are K-

function, Weighted K-function, and finally the local Gi* statistic. They are based on a

comparison (Macdonald and Small, 2009) of observed data acquired within a specified

area to a complete spatial randomness (CSR) model. We denote d as the distance

between the locations of two randomly chosen events.

A simple K-function for a specified distance d is described as

$$L(d) = \frac{\substack{\textit{Expected number of extra events}\\ \textit{within distance d of given event}}}{\lambda} \qquad (8)$$

where λ is the intensity, or the average number of events per unit area. The CSR model

for K-function is

$$L(d) = \frac{\pi d^2 \times \lambda}{\lambda} = \pi d^2 \qquad (9)$$

where the expected number of events increases linearly with the area of a circular region

with radius d around a specific event. Clustering is indicated when L(d) is larger than it

would be under the CSR Model in equation 9. The K-function focuses on the variance

or second moment of the interevent distances of the Cartesian [x, y] point anomaly

locations. It takes into account all combinations of pairs of points. The expected values

(1,2,3,4,5, etc.) in a perfectly random distribution imply that for each unit increase in

expectation, there is a unit increase in observation (e-mail communication with Arthur

Getis, 2010).

The PPA program (Alstadt,*et al.*, 2002) takes into consideration the density of points,

the borders and the size of the sample. The equation for the PPA K-function is as

follows:

$$L(d) = \sqrt{\frac{(A \sum_{i=1}^{N} \sum_{j=1,j\neq i}^{N} k(i,j))}{(\pi N(N-1))}} \qquad (10)$$

where

A is the area contained in the site

N is the number of observation ,points, or events, and

d is the inter-eventdistance

$$\sum_{i=1}^{N} \sum_{j=1,j\neq i}^{N} k(i,j)$$ is the number of j points within distance d of all i points. k(i,j) is the weight is estimated by

a. If no edge corrections,

k(i, j) =1 in case d(i, j) ≤ d or k(i, j) =0 otherwise

b. If a point is closer to one boundary than it is to a point j, the border correction is

utilized.

where e is the distance to the nearest edge.

$$k(i,j) = (1 - \frac{cos^{-1}(\frac{e}{d(i,j)})}{\pi})^{-1} \qquad (11)$$

c. If a point i is closer to two right angle boundaries than it is to point j, the weighting

equation becomes

$$k(i,j) = \{cos^{-1}(\frac{e_1}{d(i,j)}) + cos^{-1}(\frac{e_2}{d(i,j)} + \frac{\pi}{2})/(2\pi)\}^{-1}$$

e_1, e_2 are the respective distances to the nearest vertical and horizontal borders.

The PPA program is a free on-line statistical toolbox designed specifically for spatial analysis applications. It is used in this study because it contains all the statistical computer routines, including cluster analysis, needed to identify and locate anomalies of interest. The authors of the program are well known experts in their respective areas of statistical application according to the literary research conducted for this study.

This program (Figure 2) calculates the distances d(i, j) between all combinations of points and calculates $k(i, j)$ for all pairs and then calculates L(d) for all d. The program will randomly generate the N points in the whole study area M times, and estimate the minimum and maximum possible K(d) which defines the confidence envelope. The above statistical equations describe how this process is performed on the data. Each data point{x,y}for the K-function is evaluated and summed at increasing distance until the maximum search distance is reached or a border is reached. If a border is reached then border corrections are applied to the data set as shown in equations 11 and 12.
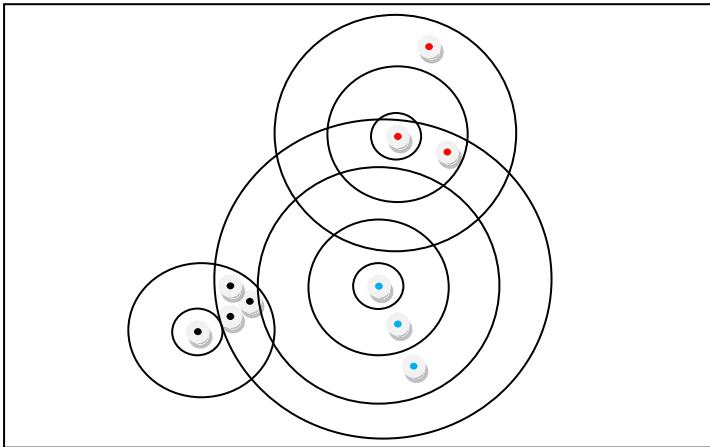
Figure 2. The PPA program identifies clustering from all points
contained in the data set area. In the small event (left radii)
clustering is evident at inter-event distance 1-2. The same cluster
is recorded at inter-event distance 3-4 for the large (center radii) event.
While the top event (red points) shows random distribution.

  Once the data are analyzed using the K-function the weighted K-function (Getis,

1982) can be used to further explore the clusters. The weighted K-function uses a 3rd

variable to indicate clustering in addition to that found by the K-function. This technique

is able to spatially filter the clusters using a physical property value ,for instance, the

millivolt readings. If the millivolt readings are used then the higher EM responses will

be favored in the search for clusters. Thus enhancing the research objective of anomaly

selection by the millivolt strength of the EM response. Another 3rd variable (Figure 3) to

consider is anomaly selection using the time decay of the EM response. The time decay

can be used to infer depth of burial and metallic volume. Long decays can generally

indicate large objects at depth. It can also infer the volumetric metal content of the

anomaly. For instance, the millivolt response can be low, but if its decay time is long,

than it becomes a more interesting anomaly because the possibility exists that it is a large

object at depth. Now, there are two variables that can be used depending on what is

being sought after in the soil. This study focuses on large buried metallic objects using

the decay time of the target.

The 3-dimensional weighted K-function [L_w(d)] equation is shown below.

$$L_w(d) = \sqrt{\frac{(A \sum_{i=1}^{N} \sum_{j=1,j\neq i}^{N} z(i) * z(j) * k(i,j))}{(\pi \sum_{i=1}^{N} \sum_{j=1,j\neq i}^{N} (z(i) * z(j)))}} \qquad (13)$$

where A is the size of the study area,

z(i) is the weight of point i,

k(i, j) is the border correction value, the same as defined for the K-function.

 All calculations for the K-function are the same except for the calculation of the

confidence envelope. For that, the program randomly assigns the Z (third variable)

values of each point to the N points M times to find the minimum and maximum L(d).
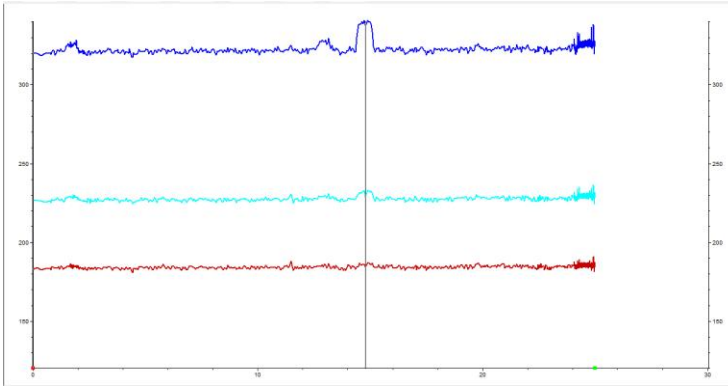
Figure 3. Diagram showing anomaly response and its
"decay to noise" as time increases. Vertical line shows
anomaly and colored horizontal lines are time gates
showing increasing time from top to bottom. This is
how the weighting is determined for Weighted K function.

The Gi-Statisics analysis provides location information. The locations of each point

{x,y} is compared to the other points in the data set. $G_i(d)$ and $G_i*(d)$ were developed

by (Ord and Getis 1995). They indicate the extent to which a location is surrounded by a

cluster of high or low values. The $G_i(d)$ statistic excludes the value at i from the

summation while the $G_i*(d)$ includes the value at i. Positive $G_i(d)$ or $G_i*(d)$ indicate

spatial clustering of high values, whereas negative $G_i(d)$ or $G_i*(d)$ indicate spatial

clustering of low values.

$$G_i(d) = \frac{\sum_{i=1,i\neq i}^{N} w_{ij}(d)x_i - \bar{x}_i \sum_{i=1,i\neq i}^{N} w_{ij}(d)}{S(i)\sqrt{\left[(N-1)\sum_{i=1,i\neq i}^{N} w_i^2(d) - (\sum_{i=1,i\neq i}^{N} w_i(d))^2\right]\Big/(N-2)}} \qquad (14)$$

where

$$\overline{x}_{,} = \frac{\sum_{i=1,i\neq}^{N} x_{,}}{N-1} \quad S(i) = \sqrt{\frac{\sum_{i=1,i\neq}^{N} x_{,}^{2}}{N-1} - (\overline{x}_{,})^{2}} \tag{15}$$

and

$$G_{i}^{'}(d) = \frac{\sum_{i=1,}^{N} w_{,,}(d)x_{,} - \overline{x}\sum_{i=1,}^{N} w_{,,}(d)}{S\sqrt{\left[N\sum_{i=1,}^{N} w_{,,}^{2}(d) - (\sum_{i=1,}^{N} w_{,,}(d))^{2}\right] \Big/ (N-1)}} \tag{16}$$

where

$$\overline{x} = \frac{\sum_{i=1,}^{N} x_{,}}{N} \quad S = \sqrt{\frac{\sum_{i=1,}^{N} x_{,}^{2}}{N} - (\overline{x})^{2}} \tag{17}$$

Both $G_{i}(d)$ and $G_{i}*(d)$ are asymptotically normally distributed as d increases.
Under the null hypothesis that there is no association between the {x, y} coordinate
points, the expectation value is 0,the variance is 1. If the underlying data are normally
distributed,we can consider their values as standard variates.

The Gi statistic is important to this research because the actual coordinates of high
and low value clusters are given in each case. For the case of decay time, if G(d) is high
(greater than 1) the anomalies with long decays are identified and located. If Gi(d) is
low (less than -1) the anomalies with short decay times are identified and located. This
ability is paramount to this research.

5. HYPOTHESIS

Lowering the false alarm rate is a major concern for those working on the remediation of UXO contaminated sites. The identification of archaeological artifacts is also an area in which the false alarm rate is very high. A method is needed to make safe recovery of UXO and the discovery of archaeological artifacts a more efficient process, keeping a high probability of detection but generating fewer false alarms.

At the San Jacinto Battleground we have surveyed 5 study sections selected according to archaeological formation process theory to be in areas located on the battle field or along the path of retreat by the Mexican Army in April of 1836. This would possibly include *deposition* of clothing and equipment during the hurried retreat. Considering the *disturbance* of those articles by farming or other animal trampling are consistent with cultural formation processes. While *nature* of moving water and *duration* of burial can be considered as forms of natural formation processes. These formation processes along with written accounts and maps guided the area selection process. Three (Area1, 2, 3) of the four study sections are rectangular 30m by 45m areas. Area A was actually the first area surveyed in 2004 and was 45m by 45m. In Area A the battery power of the EM-63 went down considerably during the last 15m of data acquisition. This prompted the reduction of the remaining Areas to 30m by 45m in 2007. The final area was the site of General Santa Anna's campsite that was a $25m^2$ area located behind the ruins of the Breastworks. We performed time domain EM-63 surveys over one 30m by 45m areas and then analyzed the data using the Point Pattern Analysis (PPA) Programs. Based on the K , Weighted K and Gi statistical subroutines, we prioritized the excavation of all the

found anomalies present. Using the information from PPA analysis and future archaeological ground truth excavations we can develop models that set criteria for anomaly selection/recovery in the subsequent study areas. The process is iterative and refined as we progress from study Area 1 to 3 ending with Area A and Santa Anna's Campsite.   In the last stage of the study, all anomalies in all 5 study areas will have to be fully excavated in order to test the predictive capabilities and objectives of the new method. To date, this has yet to be done.

5.1 Objectives

- To test the hypothesis that spatial Point Patten Analysis techniques provide information through cluster analysis about buried conductive targets associated with UXO and artifacts from historic battles.
- To develop an improved system of procedures for precisely locating and excavating buried targets on historic battlegrounds.
- To provide archaeologists with more efficient excavation strategies in order to better constrain their historical battle reconstructions.

It is predicted that most of the battle related artifacts will be accoutrements associated with the Mexican Army due to their frantic retreat from Sam Houston's forces. Artifacts of individual unit insignia and artillery ordnance such as cannonballs, rockets or grapeshot are highly valued by historical archaeologists. These artifacts are not likely to be in possession of settlers in the area and considered tangible proof of the military engagement.   Many musket balls, a horseshoe and a ramrod have been found in several

search areas at San Jacinto. They are examples of disputable provenance, however, because these are items that might be in possession the local settlers both before and after the battle.

6. METHODOLOGY

The main method of investigation for this proposal is controlled-source time domain electromagnetic induction [TDEM]. The instrument used operates in the time domain and separated into 26 geometrically spaced time gates. The instrument (Figure on page 30) is the Geonics EM-63 with a single receiver coil in the horizontal coplanar central loop configuration. The other two loops do have purpose. The top coil is the differential coil that allows the measurement of the fall-off rate of the EM response with distance from a target. This means that depth to target calculations can be used, theoretically. Practical use is not widespread. The central coil is a correction coil where the wiring is wound in the opposite direction. This is meant to counteract any fluctuations in the EM response from noise sources associated with instrument movement over terrain irregularities such as rocks, sticks or bumps from small animal burrowing.

Data were taken over specific areas, selected according to archaeological formation process theory and approved by Texas Parks & Wildlife on the San Jacinto Battleground. The main criteria for examination are large magnitude anomalies as determined by relative decay rates within the host soil. All areas that meet the criteria for further examination will be re-surveyed and subjected to the K-function statistical analysis model for cluster identification. The statistical data sets will then be compared to look for any additional information provided by the decay rates for further clustering using the Weighted K-function statistical model. The Gi statistic will be the final statistical tool used on the data to locate the points where the anomalies of interest lie.

Amateurs have had some success with hand-held instruments over the past few

decades at San Jacinto but the limitations of their instruments such as skin depth and

search methods restrain their surveys to the first 25 cm of depth. The surface coverage is

not well executed by the sweeping motions used by amateurs. On the other hand, the

EM-63 is capable of detection up to 5m under favorable conditions in conductive soil.

The survey lay-outs are engineered with total stations. Optimum surface coverage using

measuring tapes and string lines (used by masons to line up bricks) guide the EM-63

data collection lines.

Figure 4. EM-63 being used at San Jacinto Battleground.

We collected data at San Jacinto with the Geonics EM-63 electromagnetic induction

instrument (Figure 4). The last 3 areas are all 30m x 45m with the positive "Y" direction

being oriented north. Area A was 45m x 45m. The data were collected (Figure 5) from

north to south with 0.5m line spacing in a bi-directional pattern. The station spacing is

0.1m for a total of 450 readings per survey line. String lines were set out at 2 meter

intervals along the horizontal to keep them as straight as possible during the data

collection process. Operators were switched every few lines to ensure no one would

become a heat casualty due to the high heat and humidity prevalent at the site during the

late spring and summer months.
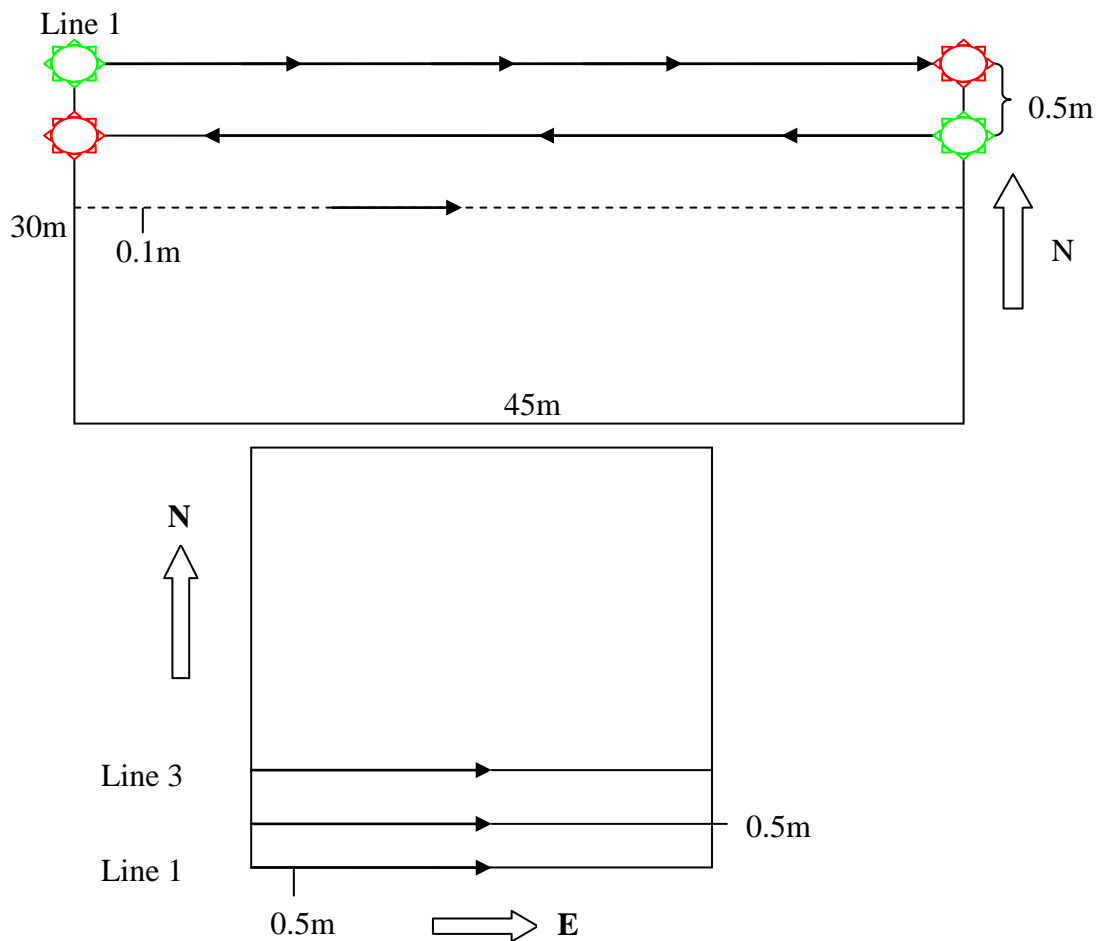
Figure 5. (a) Initial Survey layout for Em-63 data collection.
(b) Modified data collection rotocol developed at Riverside.

It should be noted that data collection with the EM-63 metal detector is difficult. The

EM-63 used in this study was operational and takes reliable data but he supporting data

acquisition and processing software supplied by the manufacture was still in the beta

testing phase (not yet released for commercial use) for this specific instrument. Data

acquisition was performed by a 3rd party data logger called the PRO 4000 manufactured

by Juniper Systems, Inc.   The data logger keypad system proved to be extremely touch

sensitive. Once a line is ready for acquisition the keypad was pressed. If the pressure

was not applied quickly and abruptly, one could start and immediately stop the line

acquisition. This also applies to changing lines, their names and directions. The

Geonics Dat63W processing software is quite intricate with a lot of operations and not

very user friendly when trying to perform data correction and editing operations. The

Dat63W correction applications such a line direction reversal are not mentioned in the

software manual and was found after hours of experimenting to happen when clicking on

the start or end indicator and dragging it to the other side of the line. Also, scale

probems arise as the program uses the line numbers for the Y scale. This can result in

area ribbons instead of rectangular areas if the scales are not of the same relative

magnitude. For instance, Y scale in tens of meters and X scale in hundreds will produce

the ribbon effect and require a lot of data editing to correct it.

Operational difficulties were also present. The EM-63 is a wheeled system with ~30

centimeters of ground clearance. The surface of the areas had to be mowed down to

accommodate this design. The mowed areas were still mottled with anthills, soil

creature burrows and small tree stumps. These inherent obstacles introduced error by

interrupting the rotation of the measurement odometer wheel. Obstacles had to be rolled over or maneuvered around if the forward progress of the EM-63 was impeded.

To alleviate a lot of the problems present using the wheel mounted configuration of the EM-63, another survey protocol (see Figure 5b) was developed at the Riverside Annex at Texas A&M University. This involves a sled mounted configuration that acquires data manually and at specified distances such as 0.5m for the new survey procedure. The lines are acquired 0.5m apart in a uni-directional pattern from west to east and begin and end at the same positions. Using this protocol, the accuracy of anomaly cluster locations is greatly improved.

Once the data collection was completed in all 5 areas (Figure 6 below) the data were processed in the Dat63W software. The data were then transferred to the SURFER 8 graphing program for visual display. The last step was to convert the data into ASCII format for input into a program (Alstadt et al., 2002) using "point pattern analysis" (PPA) statistical techniques.

Figure 6. Satellite image of areas where data were taken at San Jacinto.
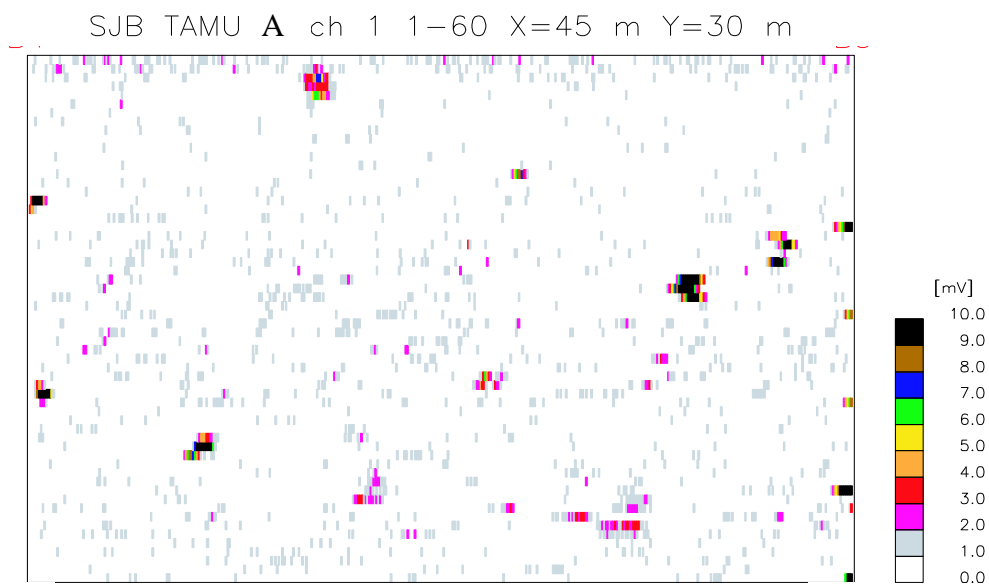
Figure 7. Plot of Area A taken in 2004 showing anomalies
and relative millivolt [mV] responses.

7. RESULTS AND ANALYSIS

Area A (Figure 7) is the site of the initial EM-63 survey conducted in September of 2004. The EM-63 survey results from Area A are analyzed qualitatively to provide a sample set of data acquisition over~$10^3 m^3$ area using a cart-mounted EM system at San Jacinto Battleground. By archaeological formation process it is assumed to be located on the historic battlefield between Sam Houston's forces and those of General Santa Ana. Formation process was assumed to be used in retrospect to this area from discussions with archaeologists who were currently working at San Jacinto. In Area A (Figure 7) we see that several targets show a large response with significant millivolt [mV] responses. These will tend to be the targets of most interest. Battle related artifacts will generally be at similar depth and in their archaeological provenience location provided they have not been disturbed geologically or by other processes.

The largest anomaly located approximately right center (X=33, Y= 16) of the plot (Figure 7) was excavated and found to be a horseshoe. The horseshoe (Figure 8) was removed hastily and the archaeological information associated with it was lost. Removal of the artifact was needed to justify to Texas Parks and Wildlife officials the need for further studies at the site.

The horseshoe is a significant find but does not provide conclusive evidence that it is associated with the battle. The radius of the shoe is small, as would be used on a cavalry horse but it could also belong to a young farming horse or a donkey for instance. This artifact is still under archaeological analysis at the present time.

Figure 8 Photo of horseshoe excavated from Area A.

Area 1 (Figure 9) shows a shaded relief of the distribution of anomalies present in a

30 m x 45 m rectangular area oriented with the positive 'Y" axis advancing north. The

darker shades indicate larger EM-63 channel 1 response values. There appears to be two

northeast-southwest elliptical trends in the anomaly distribution. These elliptical trends

could be evidence of retreat paths of the Mexican Army. The directions would be

consistent with a hurried withdrawal from the breastworks that are located ~300 m to the

north.
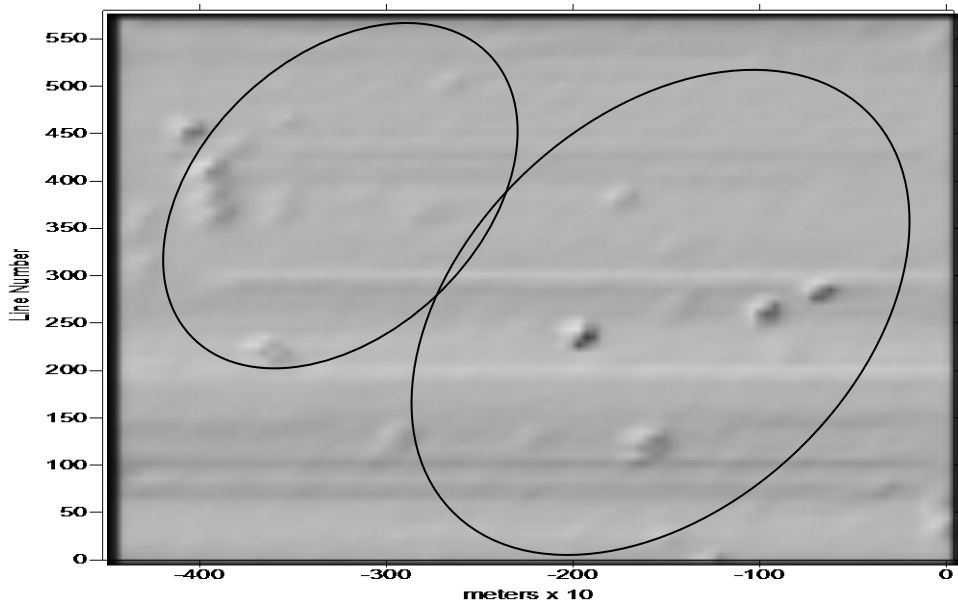
Figure 9. Shaded relief map of Area 1 showing surface anomalies.

From looking at a map (Figure 10) of the battle, Area 1 is possibly located in the path of retreat of Santa Ana's forces. The Area lies ~300 m due south of the Breastworks, see Figure 10. These were the defensive positions occupied by the Mexican forces on April 21st 1836.   Looking at a historical map of the battle the three study areas 1,2 and 3 chosen are believed to be below the bottom center cluster of trees while the fourth Area A appears to lie in the path of Colonel Lamars cavalry advance. The 5th area is the Mexican campsite directly behind the Breastworks.The map is drawn from a soldiers memory so the accuracy and scale is questionable.
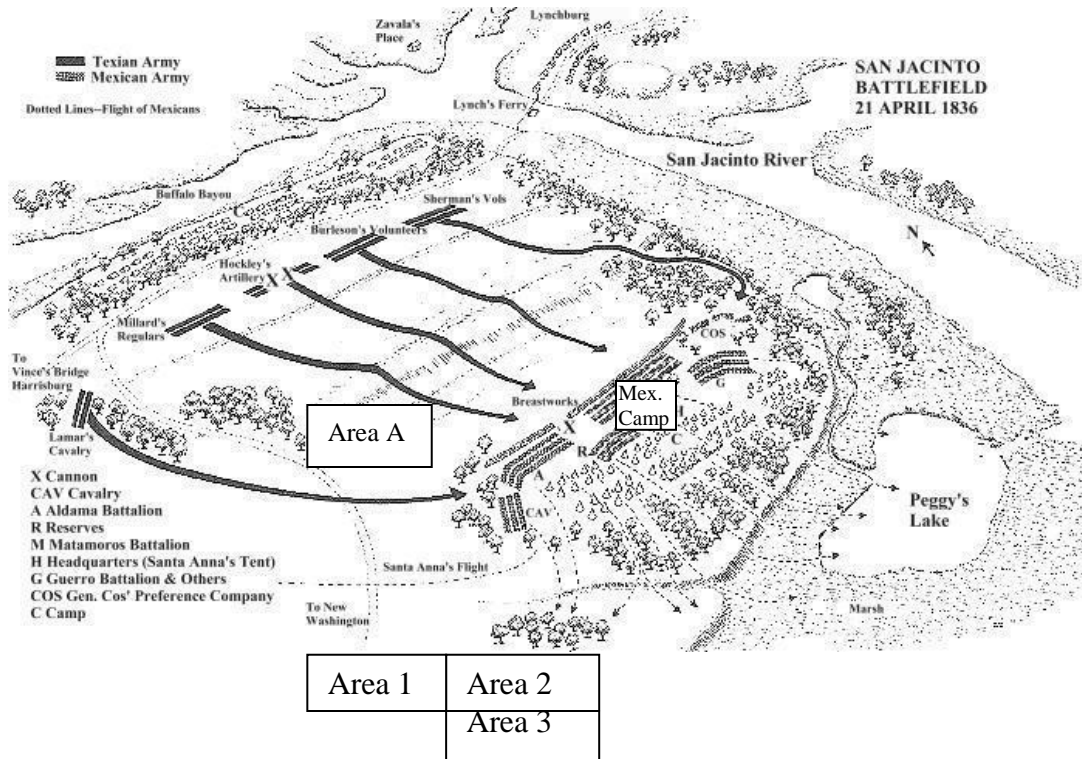
Figure 10. Map of San Jacinto Battlefield showing relative study areas
(Modified from Kendall and Hunt, 1836, contained in Hardin, 1994).

K-function analysis of the anomaly locations within Area 1 are shown in Table 1.

There is evidence of clustering from distances 1 -12. The asterisks [*] are indicative of 3

clustering criteria. There are a maximum of 3 levels or asterisks that can be classified.

The highest level is 3 asterisks and their respective orders are as follows. The first is

when the Observed L(d) is larger than the significance envelope {Maximum L(d) minus

Minimum L(d)}at a specified distance. This will be called " statistically significant

clustering."   For instance at inter-event distance 0 to 1 in Table 1 the observed L(d) is

2.81. Now 2.81 -0 = 2.81. This value is greater than the Max L(d) – Min L(d) and earns

1 asterisk. The second criteria is an Observed L(d) value at specified distance (eg.

distance 2) that is greater than Maximum L(d). The value 3.66 is greater than Max L(d)

3.27. This is also indicative of "statistically significant clustering"and earns a second

asterisk. The third criteria is an increase of an Observed L(d) value greater than 1

between distance intervals. 5.92 -4.44 is greater than 1 for inter-event distance 3-4 and

is called "secondary clustering." Secondary clustering is not statistically significant and

difficult to recognize on the graphs of L(d)-vs-Inter-event distance (Figure 11). If we

look at interval 1-2 we see that observed L(d) is 3.66 for distance 2 and 2.81 for distance

1. Now 3.66-2.81= 0.85, which is less than 1 and does not receive an asterisk for

secondary clustering.

Table 1. K-function analysis output for Area 1.

1. Observed value greater than envelope width
Stat. Sig clustering*

2. Observed value above Max L(d)
Stat Sig clustering*

3. Observed value for inter-event distance 3-4 is greater than 1
Second. clustering*

K-Function (second-order analysis)			
The input data file: **KA1.dat** (* = clustering)			
The total number of points: 40			
The minimum x coordinate: 0.00			
The maximum x coordinate: 45.00			
The minimum y coordinate: -30.00			
The maximum y coordinate: 0.00			
The total area: 1350.00			
The maximum search distance: 15.00			
The step size: 1.00			
The number of permutation for significance envelope:99			
Distance	Observed L(d)	Minimum L(d)	Maximum L(d)
1.00	2.81	0.00	2.09 ***
2.00	3.66	1.28	3.27 *
3.00	4.44	1.97	4.07 *
4.00	5.92	3.03	5.03 **
5.00	7.07	4.23	6.05 **
6.00	7.61	5.07	7.15 *
7.00	8.47	5.81	8.05 *
8.00	9.50	6.93	9.28 **
9.00	10.55	8.10	10.09 **

Table 1. continued

Distance	Observed L(d)	Minimum L(d)	Maximum L(d)
10.00	11.60	9.22	11.19 **
11.00	12.33	10.07	12.29 *
12.00	13.24	11.02	13.24 *
13.00	14.20	12.00	14.24
14.00	14.96	12.65	15.09
15.00	15.91	13.94	16.23
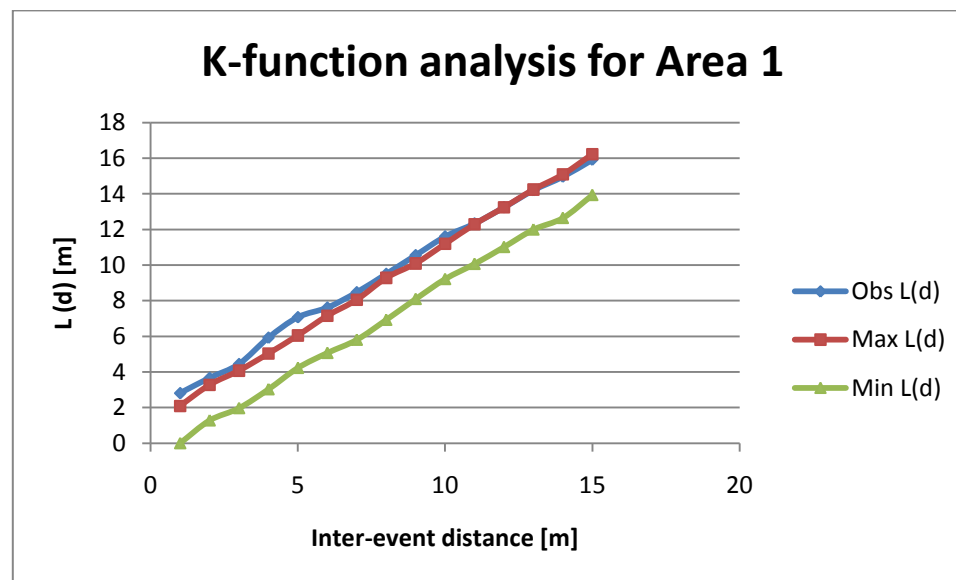
Figure 11. Showing plot of data in Table 1 for Area1. Note clustering peaks
At pts 1 and 5 on the Obs L(d) line in blue.

Applying a low cut filter to the data at a threshold of 15 mV in Area 1 (Table 2)

results in the disappearance of many of the clusters. The larger magnitude anomalies

survive the filtering process and limit the number of anomalies that need to be

excavated. The results show that there are problems with this approach. The number of

points available for analysis, after the low-cut filter, is only 23 points out of the original

40. This corresponds to a reduction in the data density by nearly 50% making the low

cut filtering process unacceptably restrictive.   After low-cut filtering only the inter-event

distance intervals 0-1, 1-2, and 3-4 still exhibit clustering above the significance

envelope. The effect of the low-cut filtering is to reduce large clustering at large inter-

event distances. This would indicate that the distribution of artifacts is only at small

inter-event distances that may not be the case at all.

Table 2. Showing K-function for Area 1 at 15mV threshold.

K-Function (second-order analysis)		
The input data file: **KA1th15.dat**		
The total number of points: **23**		
The minimum x coordinate: 0.00		
The maximum x coordinate: 45.00		
The minimum y coordinate: -30.00		
The maximum y coordinate: 0.00		
The total area: 1350.00		
The maximum search distance: 15.00		
The step size: 1.00		
The number of permutation for significance envelope:99		
Distance Observed L(d)	Minimum L(d)	Maximum L(d)
1.00 3.71	0.00	2.61 ***
2.00 4.89	0.00	4.12 **
3.00 5.23	0.00	4.64 *
4.00 6.69	2.26	5.95 **
5.00 7.38	2.97	6.87 *
6.00 7.38	4.53	7.80
7.00 7.72	5.37	8.43
8.00 8.70	6.46	9.54
9.00 10.03	7.35	10.51
10.00 11.79	8.62	11.96
11.00 12.40	9.68	13.05
12.00 12.78	10.13	14.09
13.00 13.97	11.44	15.01
14.00 14.49	12.51	15.87
15.00 15.06	13.30	16.65

.

There are some lessons to be learned from response magnitude low cut filtering. First, there is a significant loss of data density. This reduces the amount of clustering by widening the significance envelope. The K-function analysis is less robust when using a reduced number of data as indicated by the repeated Min L(d) values. The significance envelope grows in this case because Min L(d) remains at 0 for three inter-vent distances 0-1,1-2, and 2-3 while Max L(d) increases. The envelope should be kept as narrow as possible in order to achieve clustering. Both values Min and Max L(d) should increase at the same time, but not necessarily by the same amount.

Table 3. Weighted K-function output using millivolt response for Area 1.

Weighted K-Function analysis			
The input data file: **WKA1.dat**			
The total number of points: 40			
The minimum x coordinate: 0.00			
The maximum x coordinate: 45.00			
The minimum y coordinate: -30.00			
The maximum y coordinate: 0.00			
The total area: 1350.00			
The maximum search distance: 15.00			
The step size: 1.00			
The number of permutations for the confidence envelope:99			
Distance	Observed L(d)	Minimum L(d)	Maximum L(d)
1.00	3.75	1.84	3.92 **
2.00	4.33	2.77	5.10 *
3.00	5.20	3.39	6.05
4.00	6.40	4.47	7.36 *
5.00	7.15	5.60	8.93
6.00	7.48	6.37	9.72
7.00	7.91	6.87	11.00
8.00	9.08	8.23	12.23
9.00	9.87	9.30	12.96
10.00	11.09	10.07	13.82 *
11.00	11.61	10.73	14.79

Table 3. continued			
Distance	Observed L(d)	Minimum L(d)	Maximum L(d)
12.00	12.40	11.82	15.65
13.00	13.28	12.48	16.31
14.00	14.17	13.68	16.58
15.00	14.93	14.57	17.37

The next step is to input all Area 1 data into the Weighted K-function statistical

analysis. The Weighted K-function takes into account the EM63 channel-1 response

value in mV assigned to each point (x, y). As shown in Table 3 the amount of clustering

present (indicated by 2 asterisks) diminishes to the 0-1 distance at most. The results are

inconclusive with regards to the original data in Table 1. There seems to be only

secondary clustering (indicated by 1 asterisk), at best, beyond distance 2.

The next analysis procedure was to repeat the Weighted K-function technique using

the geometrically spaced EM-63 time decay gates. The time gates are used   because

they represent a decay time value that can infer depth of burial qualitatively, also the

same for metallic volume. The scale-range is smaller,1-26 timegates as opposed to 1-300

mV for the EM-63 Channel-1scale. This has the added benefit of being more sensitive

when performing the statistical analyses on the data.

We can see in Table 4 that we have significant correlation in comparison with Table 1.

At distances 0-1, we have major clustering. At distances 3-4 and 4-5 we have

statistically significant clustering and secondary clustering at distances 5-6 and 6-7.

These results suggest that using the decay time gates as the weighted 3rd dimension

corroborates best with the 2-dimensional K-function analysis in Table 1. This result

shows a stronger relationship to the K-function cluster analysis for large metallic objects

at depth giving an indication of the importance of the clusters that survive in the

weighted K-function using time gates. The result has prioritized the surviving clusters

and indicates clustering that can be considered for excavation.

Table 4. Showing better correlation with table 1 for Area 1.

Weighted K-Function analysis			
The input data file: **WKDKA1.dat**			
The total number of points: 40			
The minimum x coordinate: 0.00			
The maximum x coordinate: 45.00			
The minimum y coordinate: -30.00			
The maximum y coordinate: 0.00			
The total area: 1350.00			
The maximum search distance: 15.00			
The step size: 1.00			
The number of permutations for the confidence envelope:99			
Distance	Observed L(d)	Minimum L(d)	Maximum L(d)
1.00	3.89	2.22	3.89 ***
2.00	5.33	3.01	5.33 **
3.00	6.14	3.61	6.14 *
4.00	7.60	4.78	7.60 **
5.00	8.63	5.82	8.63 **
6.00	9.02	6.53	9.02 *
7.00	9.87	7.43	9.87 *
8.00	10.63	8.42	10.89
9.00	11.38	9.75	11.63
10.00	12.20	10.73	12.53
11.00	12.75	11.46	13.26
12.00	13.60	12.36	14.23
13.00	14.38	13.39	15.12
14.00	15.15	14.18	15.86
15.000	15.90	15.23	16.81
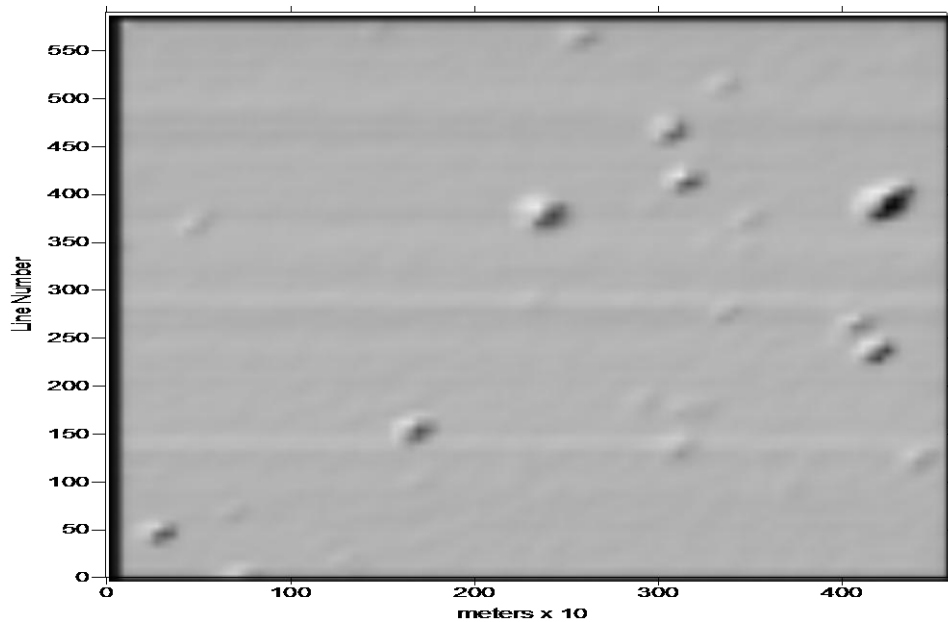
Figure 12. Shaded relief map showing anomaly locations within Area 2.

Area 2 is possibly in the path of retreat of Santa Ana's forces. It is juxtaposed to the east of Area 1. The data distribution (Figure 12) on a shaded relief image appears to be spatially random. Upon closer inspection, the data points are concentrated on the upper right side of the area. The darker locations indicate larger EM response magnitudes.

If we look at the K-function PPA output (Table 5) of Area 2 there is major clustering at the short inter-event distance 0-1 m. Statistically significant clustering appears at 1-2 and 2-3 m. There is only secondary clustering at distances 6-7, 7-8, 8-9, 10-11, 11-12, 12-13 and 14-15m. It should be noted here that secondary clustering has the least significance of the 3 classifications mentioned earlier and though secondary clustering appears at may inter-event distances they are of minor consequence.

Table 5. K-function analysis of Area 2.

K-Function (second-order analysis)			
The input data file: **KA2.dat**			
The total number of points: 49			
The minimum x coordinate: 0.00			
The maximum x coordinate: 45.00			
The minimum y coordinate: -30.00			
The maximum y coordinate: 0.00			
The total area: 1350.00			
The maximum search distance: 15.00			
The step size: 1.00			
The number of permutation for significance envelope:99			
Distance	Observed L(d)	Minimum L(d)	Maximum L(d)
1.00	2.77	0.00	2.00 ***
2.00	3.73	1.19	2.68 *
3.00	4.14	2.11	3.67 *
4.00	4.62	3.05	4.81
5.00	5.13	4.28	5.87
6.00	5.65	5.17	6.89
7.00	6.99	6.20	7.69 *
8.00	8.44	7.16	8.87 *
9.00	9.50	7.93	10.25 *
10.00	10.35	9.00	11.25
11.00	11.56	9.98	12.26 *
12.00	12.74	10.87	13.48 *
13.00	13.93	12.12	14.74 *
14.00	14.84	12.88	15.83
15.00	16.20	13.86	16.85 *

   Since it was found that magnitude filtering was not informative, after the Area 1

analysis, the next step is to perform a weighted cluster analysis. This involves taking 2-

dimensional K-function data and transforming them it into 3-dimensional data using the

[mV] response. The Weighted K-function approach uses the EM-63 response [mV]

magnitudes at each point. The results of this analysis are shown in Table 6 below.

Table 6. Weighted K-function analysis of Area 2 using [mV] readings.

Weighted K-Function analysis			
The input data file: **WKA2.dat**			
The total number of points: 49			
The minimum x coordinate: 0.00			
The maximum x coordinate: 45.00			
The minimum y coordinate: -30.00			
The maximum y coordinate: 0.00			
The total area: 1350.00			
The maximum search distance: 15.00			
The step size: 1.00			
The number of permutations for the confidence envelope:99			
Distance	Observed L(d)	Minimum L(d)	Maximum L(d)
1.00	4.60	1.90	4.18 ***
2.00	5.32	2.44	4.98 *
3.00	5.59	2.87	5.54 *
4.00	5.86	3.01	6.39
5.00	6.36	3.48	6.52
6.00	6.56	4.19	6.68
7.00	7.66	5.39	7.91 *
8.00	9.10	6.48	9.58 *
9.00	10.84	7.25	11.23 *
10.00	11.34	7.84	12.07
11.00	12.37	8.67	12.72 *
12.00	13.54	9.52	14.03 *
13.00	15.05	10.48	15.25 *
14.00	16.18	11.18	16.19 *
15.00	17.27	13.30	17.53 *

Using the [mV] responses there is major clustering at distance 0-1 m. There is

statistically significant clustering at distance 1-2 and 2-3m because they appear above

the confidence envelope, that is, Observed L(d) is greater than Maximum L(d).

Secondary clustering is indicated at distances 6-7, 7-8, 8-9, 10-11, 11-12-13, 13-14 and

14-15. The 0-1, 1-2 and 2-3 distances correlate well with Table 5. This means that the

clusters mentioned survive the weighted K-function analysis using the mV values and

match well with the clusters indicated in Table 5.

Table 7. Weighted K-function of Area 3 using decay time

Weighted K-Function analysis			
The input data file: **WKDKA2.dat**			
The total number of points: 49			
The minimum x coordinate: 0.00			
The maximum x coordinate: 45.00			
The minimum y coordinate: -30.00			
The maximum y coordinate: 0.00			
The total area: 1350.00			
The maximum search distance: 15.00			
The step size: 1.00			
The number of permutations for the confidence envelope:99			
Distance	Observed L(d)	Minimum L(d)	Maximum L(d)
1.00	3.91	2.18	3.39 ***
2.00	5.28	2.93	4.31 **
3.00	5.43	3.62	4.84 *
4.00	5.63	4.04	5.43 *
5.00	5.90	4.54	5.87 *
6.00	6.29	4.96	6.42
7.00	7.64	6.11	7.70 *
8.00	9.21	7.58	9.28 *
9.00	10.38	8.31	10.54 *
10.00	11.20	9.16	11.39
11.00	12.38	10.43	12.54 *
12.00	13.48	11.60	13.80 *
13.00	14.66	12.79	15.04 *
14.00	15.55	13.69	16.01
15.00	16.75	15.19	17.17 *

Table 7 shows the Weighted K-function over Area 2. The weighted variables are

changed for this analysis. In this analysis the variables used are the decay time gates

associated with the anomaly point locations to see if the time gate variable shows better

correlation to Table 5 than the weighted K mV analysis in Table 6. From the data listed in Table 7 we can see major clustering at distance 0-1m. Distances 1-2, 2-3, 3-4 and 4-5 m indicate statistically significant clustering. Note at distance 1-2 we have statistically significant clustering that is borderline major clustering because it is only 0.01 smaller than the envelope width. Secondary clustering is prevalent beyond distance of 6 m or greater. They are located at distances 6-7,7-8, 8-9, 10-11,11-12, 12-13 and 14- 15 m.
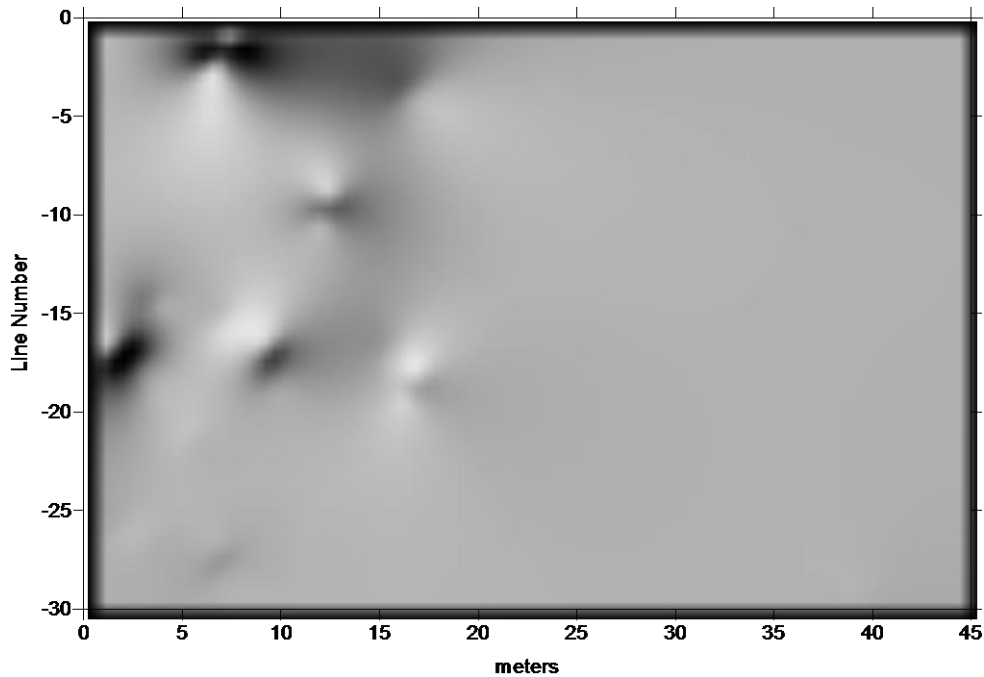

Figure 13. Shaded relief map of Area 3 showing anomaly locations.

Area 3 (Figure 13) is juxtaposed to the south of Area 2. This area is also believed to be on the retreat path of the Mexican army according to the battle historical map shown earlier. The anomaly locations appear to be concentrated on the left side of the shaded relief map.

Table 8. K-function analysis of Area 3.

K-Function (second-order analysis)			
The input data file: **KA3.dat**			
The total number of points: 37			
The minimum x coordinate: 0.00			
The maximum x coordinate: 45.00			
The minimum y coordinate: -30.00			
The maximum y coordinate: 0.00			
The total area: 1350.00			
The maximum search distance: 15.00			
The step size: 1.00			
The number of permutation for significance envelope:99			
Distance	Observed L(d)	Minimum L(d)	Maximum L(d)
1.00	2.98	0.00	2.40 ***
2.00	4.644	0.80	3.34 **
3.00	5.08	1.39	4.09 *
4.00	6.29	2.94	4.87 **
5.00	7.15	4.21	6.08 *
6.00	8.48	4.96	6.79 **
7.00	10.01	5.77	7.78 **
8.00	11.34	6.88	8.77 **
9.00	12.28	7.95	9.86 *
10.00	13.76	9.15	11.09 **
11.00	15.03	10.13	12.14 **
12.00	16.29	10.79	13.01 **
13.00	17.47	11.98	14.16 **
14.00	19.16	12.83	15.35 **
15.00	20.14	14.00	16.41 *

The K-function analysis for Area 3 (Table 8) indicates major clustering at distance 0-1 m. Statistically significant clustering is shown at all distances 0-15 m. Secondary clustering is evident at distances 1-2, 3-4, 5-6, 6-7, 7-8, 9-10, 10-11, 11-12, 12-13 and 13-14 m. There are many inter-event distances that are of statistical significance.

Table 9. Weighted K-function analysis of Area 3 using [mV] magnitudes.

Weighted K-Function analysis			
The input data file**: WKA3.dat**			
The total number of points: 37			
The minimum x coordinate: 0.00			
The maximum x coordinate: 45.00			
The minimum y coordinate: -30.00			
The maximum y coordinate: 0.00			
The total area: 1350.00			
The maximum search distance: 15.00			
The step size: 1.00			
The number of permutations for the confidence envelope:99			
Distance	Observed L(d)	Minimum L(d)	Maximum L(d)
1.00	9.02	1.35	9.02 *
2.00	11.27	2.80	11.27 *
3.00	11.30	2.97	11.30
4.00	11.59	4.31	11.59
5.00	11.75	4.39	11.75
6.00	11.93	6.15	12.07
7.00	12.13	6.96	13.63
8.00	12.77	7.66	15.34
9.00	13.31	8.88	16.16
10.00	15.41	10.03	17.51 *
11.00	18.05	12.39	18.24 *
12.00	18.38	13.11	19.57
13.00	18.75	13.84	20.85
14.00	19.79	15.28	22.45 *
15.00	20.04	15.73	23.53

Continued analysis of Area 3 using the Weighted K-function with the [mV] magnitudes

are shown in Table 9.   In this analysis there is no major clustering in the 0-1 m

distance. In fact there is only secondary clustering at distances 0-1, 1-2, 9-10, 10-11 and

13-14 m. Of interest is that the distances 0-5m are all on the envelope (Observed L(d) =

Max L(d)). By being on the envelope they are down graded to secondary clustering.

Another interesting observation is the envelope width (Max L(d) – Min L(d)) is approximately 7.5 as compared to 2.5 for Table 5. The envelope widths do not correspond well, the envelope is wider for Table 9 and therefore there will be less statistically significant.

The Weighted K-function analysis for Area 3 using the decay time gates yields the values in Table 10. There is again no major clustering at distance 0-1 m. There is, however, statistically significant clustering at distances 0-1 and 1-2 m. Secondary clustering is present at distances 5-6, 6-7, 7-8, 9-10, 10-11, 11-12 and 13-14 m. The envelope width (~2 m) is also comparable to the envelope width (~2.5) in Table 8.

With the analysis of the data taken from Areas 1, 2 and 3 in 2007 there seems to be an emerging relationship between the 2 dimensional K-function analysis and the 3-dimensional Weighted K-function analysis using decay time gates. To further test this emerging relationship, the data from Area A (Figure 14) in 2004 was also analyzed in the same manner for completeness.

Table 10. Weighted K-Function analysis of Area 3 using decay time gates.

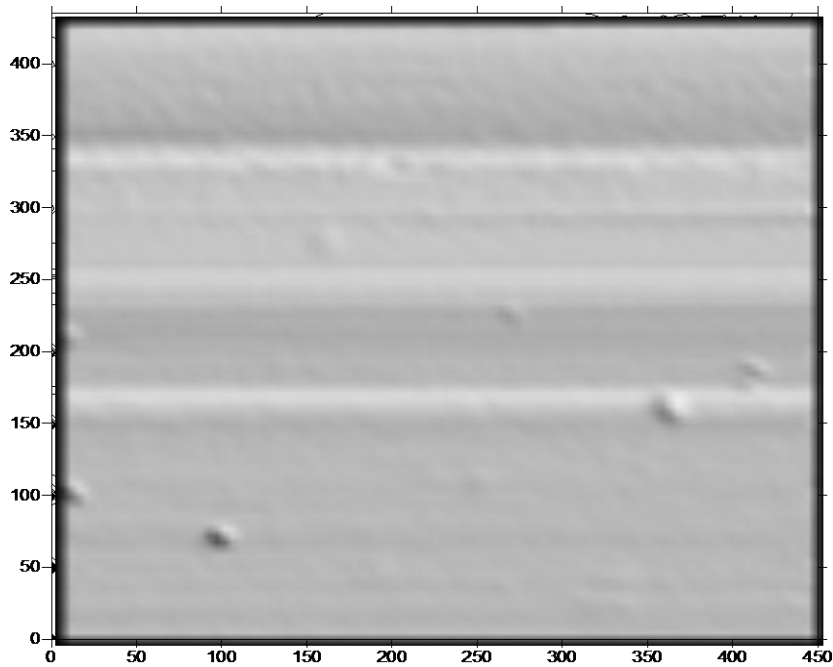| Weighted K-Function analysis			
The input data file: **WKDKA3.dat**			
The total number of points: 37			
The minimum x coordinate: 0.00			
The maximum x coordinate: 45.00			
The minimum y coordinate: -30.00			
The maximum y coordinate: 0.00			
The total area: 1350.00			
The maximum search distance: 15.00			
The step size: 1.00			
The number of permutations for the confidence envelope:99			
Distance	Observed L(d)	Minimum L(d)	Maximum L(d)
1.00	4.00	2.39	4.01 *
2.00	6.28	4.18	6.30 *
3.00	6.51	4.29	6.54
4.00	7.26	5.46	7.28
5.00	7.88	6.18	8.32
6.00	8.97	7.62	9.98 *
7.00	10.10	9.12	11.22 *
8.00	11.28	10.28	12.35 *
9.00	12.03	11.29	13.26
10.00	13.73	12.78	14.82 *
11.00	15.47	14.06	15.97 *
12.00	16.55	15.35	17.51 *
13.00	17.43	16.25	18.79
14.00	18.95	17.65	20.39 *
15.00	19.71	18.85	21.22

Figure 14. Shaded relief map of Area A.

Table 11. K-function analysis of Area A taken in 2004.

K-Function (second-order analysis)			
The input data file: **KAA.dat**			
The total number of points: 35			
The minimum x coordinate: 0.00			
The maximum x coordinate: 45.00			
The minimum y coordinate: 0.00			
The maximum y coordinate: 45.00			
The total area: 2025.00			
The maximum search distance: 22.00			
The step size: 1.00			
The number of permutation for significance envelope:99			
Distance	Observed L(d)	Minimum L(d)	Maximum L(d)
1.00	3.79	0.00	2.32 ***
2.00	4.94	0.00	3.12 ***
3.00	5.50	1.12	4.43 *
4.00	6.32	2.54	5.11 *
5.00	7.34	3.82	5.82 **
6.00	7.70	4.87	6.95 *
7.00	8.27	5.75	8.35

Table 11. continued

Distance	Observed L(d)	Minimum L(d)	Maximum L(d)
8.00	8.89	6.71	9.19
9.00	9.94	7.83	10.46 *
10.00	11.66	8.89	11.47 **
11.00	12.73	9.64	12.47 **
12.00	14.10	10.66	12.93 **
13.00	16.21	11.71	14.04 **
14.00	16.86	12.42	15.58 *
15.00	17.71	13.20	16.90 *
16.00	18.84	14.29	17.80 **
17.00	19.88	15.31	18.75 **
18.00	20.46	16.37	19.53 *
19.00	21.53	17.49	20.58 **
20.00	22.24	18.43	21.93 *
21.00	23.28	19.36	22.73 **
22.00	23.90	20.44	23.75 *

The Area A data is shown in Table 11 above. Area A is larger than the other 3 areas being 45m x 45m. The K function analysis shows major clustering at distances 0-1 and 1-2 m. Statistically significant clustering at distances 4-5, 9-10, 10-11, 11-12, 12-13, 15-16, 16-17, 18-19 and 20-21 m. Secondary clustering appears at distances 2-3, 3-4, 5-6, 8-9, 13-14, 14-15, 17-18, 19-20 and 21-22 m.

Table 12 displays the Weighted K-function of Area A using the millivolt [mV] magnitudes as the weighting factor. The analysis shows no major or statistically significant clustering. There is only secondary clustering at distances 0-1, 2-3, 9-10, 11-12, 12-13, 15-16, 16-17, 17-18, and 18-19m. There is only minor correlation with Table 11 at best using the [mV] readings.

Table 12. Weighted K-function analysis from Area A using [mV] Readings.

Weighted K-Function analysis			
The input data file: **WKAA.dat**			
The total number of points: 35			
The minimum x coordinate: 0.00			
The maximum x coordinate: 45.00			
The minimum y coordinate: 0.00			
The maximum y coordinate: 45.00			
The total area: 2025.00			
The maximum search distance: 22.00			
The step size: 1.00			
The number of permutations for the confidence envelope:99			
Distance	Observed L(d)	Minimum L(d)	Maximum L(d)
1.00	3.51	1.25	11.44 *
2.00	4.13	2.55	11.95
3.00	5.24	2.91	11.98 *
4.00	5.48	3.15	12.04
5.00	6.06	3.60	14.18
6.00	6.23	3.71	14.20
7.00	6.30	4.14	14.29
8.00	6.66	4.42	14.36
9.00	7.15	5.28	15.97
10.00	9.52	6.05	18.15 *
11.00	9.85	6.82	18.30
12.00	11.28	7.74	19.16 *
13.00	13.59	9.38	21.65 *
14.00	13.72	9.73	21.71
15.00	13.87	10.54	22.30
16.00	15.53	10.85	26.13 *
17.00	16.89	11.40	26.82 *
18.00	18.42	11.68	27.02 *
19.00	22.03	12.17	28.36 *
20.00	22.10	12.57	28.46
21.00	22.35	14.42	28.74
22.00	22.73	14.68	28.86

Table 13. Weighted K-function analysis from Area A using decay time gates.

Weighted K-Function analysis			
The input data file: **WKDKAA.dat**			
The total number of points: 35			
The minimum x coordinate: 0.00			
The maximum x coordinate: 45.00			
The minimum y coordinate: 0.00			
The maximum y coordinate: 45.00			
The total area: 2025.00			
The maximum search distance: 22.00			
The step size: 1.00			
The number of permutations for the confidence envelope:99			
Distance	Observed L(d)	Minimum L(d)	Maximum L(d)
1.00	4.82	2.85	5.29**
2.00	5.66	4.06	6.23
3.00	6.29	4.47	6.79
4.00	6.90	4.94	7.81
5.00	8.02	5.90	8.94*
6.00	8.72	6.52	9.25
7.00	8.93	6.95	9.34
8.00	9.48	7.52	10.02
9.00	10.25	8.68	11.18
10.00	11.29	10.13	13.61*
11.00	11.81	10.72	14.42
12.00	13.78	12.47	16.66*
13.00	16.08	14.63	18.46*
14.00	16.71	15.35	18.98
15.00	17.49	15.89	19.75
16.00	18.50	17.31	20.73*
17.00	19.27	18.32	21.77
18.00	19.95	19.11	22.26
19.00	21.51	19.79	23.12*
20.00	21.91	20.40	23.95
21.00	22.54	20.90	24.77
22.00	23.09	21.71	25.31

The last analysis conducted is to perform a weighted K-function analysis of the data from Area A into the Weighted K-function program. This time the weighted variables are the decay time gates at each position.   To see if there is better correlation with the K-function analysis in Table 11. The results are displayed in Table 13. There now appears to be some correlation present since there is statistically significant clustering at distance 0-1m. Secondary clustering appears at distances 4-5, 9-10, 11-12, 12-13, 15-16 and 18-19 m. One could argue that there is only one inter-event distance of interest. This would seem to indicate an insignificant amount of clustering result but if we compare the significance envelope widths from both Weighted K function results we see that the results using the decay time gates is also more comparable to the K-function analysis in Table 11.

Use of K and Weighted K function are shown in this analysis to segregate and prioritize the anomalies present. Unfortunately, they do not provide any location information to guide us to the anomalies of greatest interest. Location information will be needed to satisfy some of the primary objectives set forth in this study.

Archaeological interests in this type of work include the prioritization of clusters and their relative inter-event distances. For cultural formation processes clustering at short inter-event distances can translate to artifacts in the systemic record in relation to the battle. This could be by *deposition* of Mexican uniform insignia, military paraphernalia, and clusters of musket balls dropped by fleeing soldiers. Clustering at long inter-event distances translates to items that have undergone *disturbance* from farming, animal or

other anthropogenic activities that have served to separate the anomalies in the

archaeological context.

For natural formation processes short inter-event distances could come from *nature*.

Moving water would be able to gather artifacts in a natural depression in the soil. Once

there the time of burial, or *duration,* could have an additive or subtractive *effect*

depending on the chemical content in the moving water. Moving water could also

disperse artifacts which would be indicated by long inter-event distances in the statistical

analysis thereby affecting the *scale*.

Table 14. Gi* Statistic for Area 1 indicating specific excavation locations.

Local Gi *Statistic for Area 1		
The input data file: **GA1DK.dat**		
The total number of points: 40		
Distance: 1.00 m		
# Position (x,y)	Gi*(d)	
1 (0, 0)	**0.00**	**No artifact selected**
2	0.00	
3	0.00	
4 (3.5, -4.5)	**1.92**	**Lower level important artifact**
5	1.33	
6	0.00	
7	2.27	
8 (4.9, -7.5)	**3.53**	**Most important artifact**
9	2.61	
10	0.00	

An example of the output (Table 14) for the Gi* Statistic is shown below for Area 1.

This is a portion of the output that shows the first ten positions in Cartesian coordinates

{x,y}. This analysis shows the locations of clustering at distance 0-1 of each individual

point. From the data shown, point #8 located at (x=4.9m, y=-7.5m) to be the anomaly of

most interest in Area 1. We now have an analysis procedure that enables us to locate

specifically the anomalies that are most likely to be UXO or archaeological artifacts.

 Using the modified data collection technique developed at the Riverside Annex at

Texas A&M University we can compare the data quality to the initial data collection

technique and clearly see the improvements in the DAT63W program displays shown in
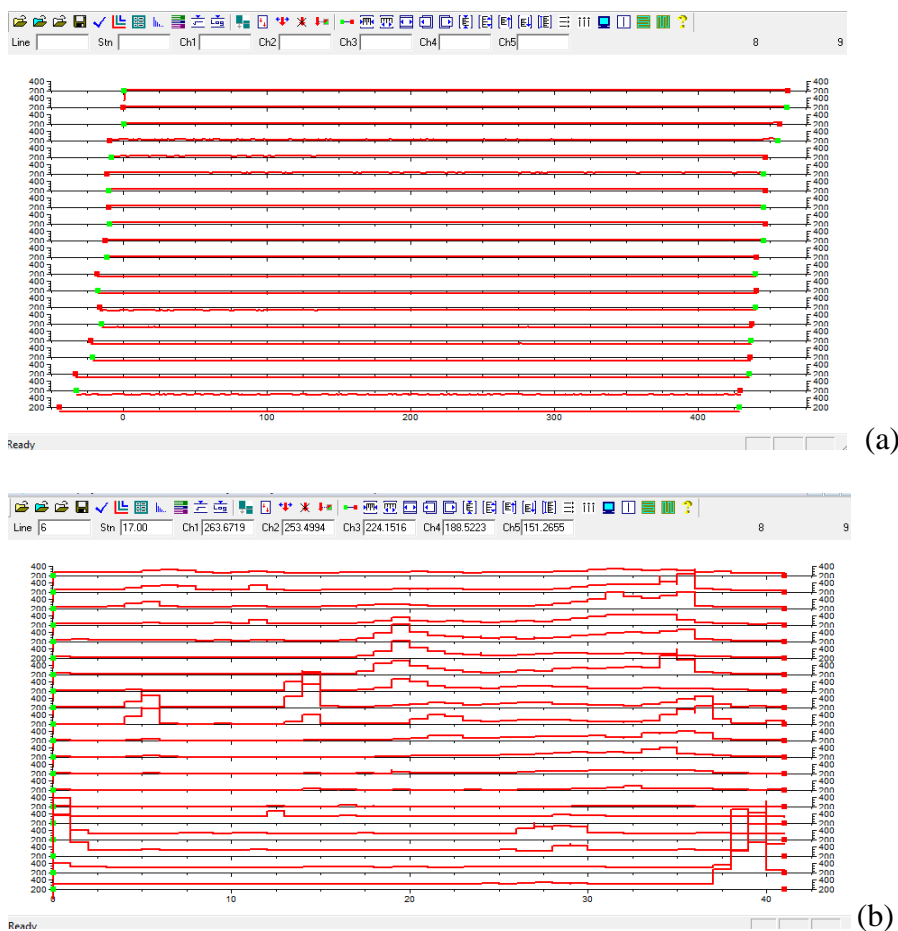
Figure 15a and 15b below.

(a)

(b)

Figure 15. (a) Initial raw survey results from Area A notice
the cumulative error (drift) and irregular line distances.
(b) Raw survey results from data taken at Riverside Annex
 using modified survey strategy.

The bi-directional survey indicated by the alternating green and red dots a the ends of the the lines in Figure 15a shows need for quite a bit of editing in the DAT63W program to correct for position. Figure 15b is uni-directional and requires no positional editing in the DAT63W program because there is no cumulative error and all lines begin and end in the same positions. While this technique takes more time to collect the data. The trade-off between data collection time and post processing saves more time in the long run because data editing for positional accuracy is a much longer process than adjusting the data collection procedure. Data editing for position has a low degree of confidence. Adjusting survey procedures ensures hi accuracy of anomaly locations and was incorporated into the data collection procedures on the Mexican Army Campsite at San Jacinto Battleground. The resulting data sets were easier to interpret and had a high degree of confidence with respect to artifact location.

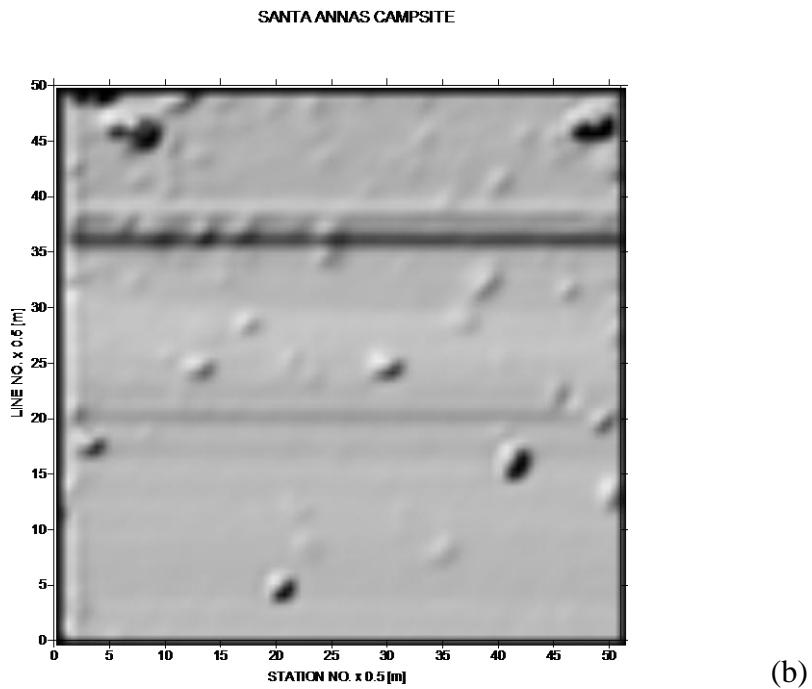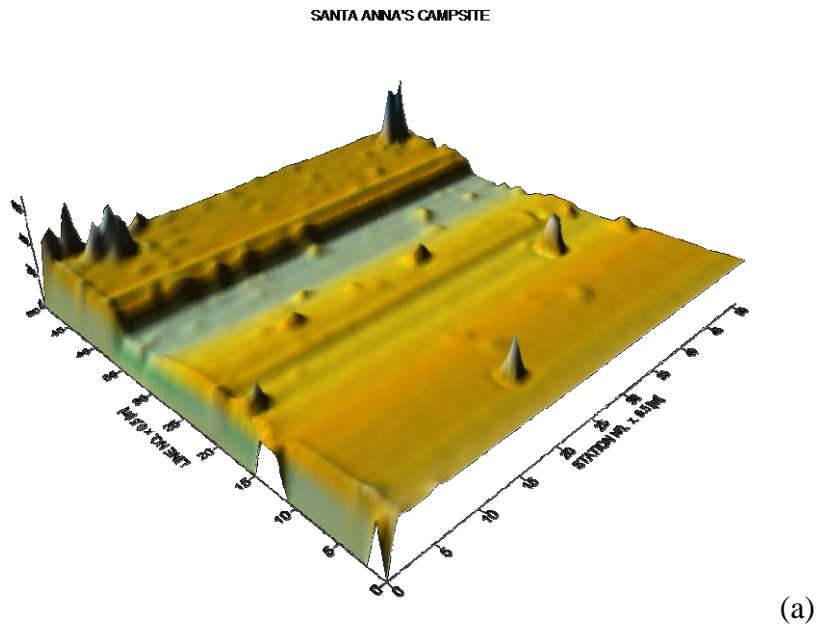SANTA ANNA'S CAMPSITE

(a)

SANTA ANNAS CAMPSITE

(b)

Figure 16. (a) Surface map of Mexican Campsite generated in Surfer 8 from the channel-1 mV responses. (b) Shaded relief map of same site showing anomaly locations.

7.1 Mexican Campsite

The data collection at the Mexican campsite is of very high quality. The campsite is shown (Figure 16a and b) in a surface map and a shaded relief map above . Both maps clearly show the anomalies located within the $25m^2$ area. The linear depressions on the surface map are matched with the horizontal lines on the shaded relief map. The major depression and large horizontal line located at $Y = 36$ were a result of a battery change. The smaller depressions and lines indicate a personnel switch after a brief break that allowed the internal electronics of the EM-63 to cool before resuming data collection.

K-function analysis of the Campsite (Figure 17) shows clustering at almost all distances except distance 0-1m. This would be consistent with a former occupied campsite where objects have been dropped or discarded.
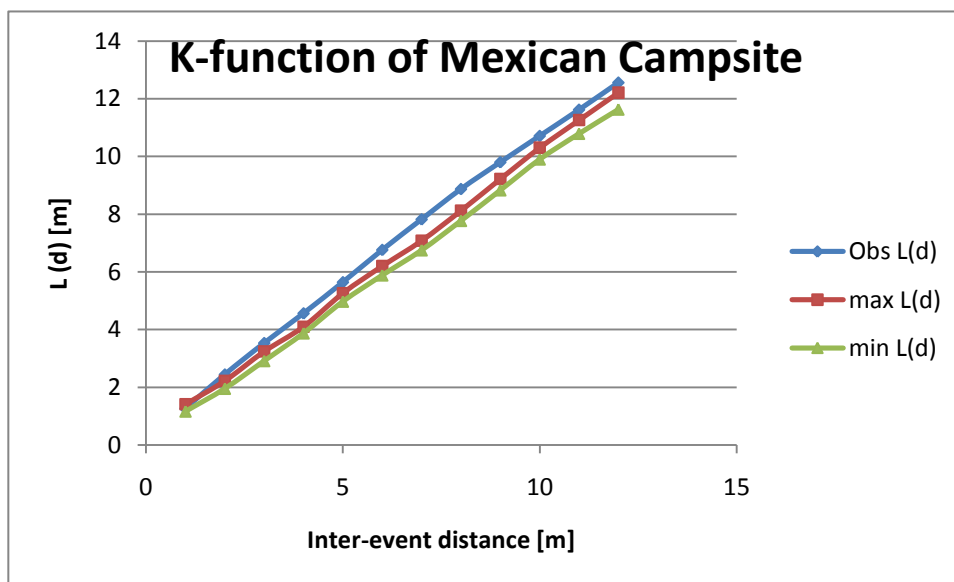

Figure 17 K-function showing clustering at many distances within campsite.

When put through the weighted K-function (Figure 18) using time decay the data still shows clustering at distances 0-1, 1-2, 7-8, 8-9, 9-10, and 10-11. It is difficult to see from the graph but the weighted K confirms the presence of significant buried metallic objects on this site and warrants further examination using the Local Gi* Statistical analysis.
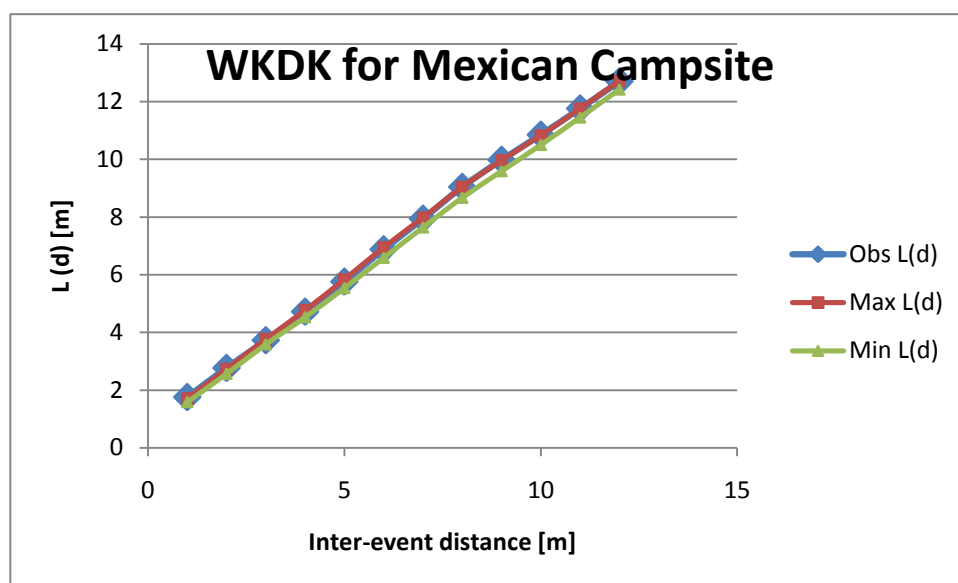

Figure 18. Weighted K-function confirming presence of prominent artifacts.

The Local Gi Statistical analysis provides a list of the coordinates of the actual anomaly cluster members and an assigned numerical value that can be both positive and negative. The anomalies here are specifically targeted to be large buried metallic artifacts within a cluster based on their decay to noise rates. For this analysis, the positve numbers are desired from largest to smallest but no smaller than +1 because the

variance is -1 to +1. The larger positive numbers have a greater priority than the lower

numbers and are sorted into a "Dig List" as shown in Table 15 for the Mexican Campsite

Table 15. Dig List of anomalies selected by decay rates.

Santa Anna Camp Priority Dig List

Gi*Stat Value	x-coord [m]	y-coord [m]
5.19	24.2	23.5
4.89	23.8	23
4.51	1	25
3.86	24.2	24
3.83	24.5	23
3.62	1.4	24.5
3.49	0.5	24.5
3.42	25.2	23.5
3.42	0.4	25
3.11	2	25
2.98	12.2	18
2.83	25.3	12.5
2.69	19.5	16.5
2.54	12.3	18.5
2.35	23.2	22.5
2.25	16.8	4
2.25	17.7	4
2.25	17.5	4.5
2.25	12	17.5
2.12	24.9	12
2.12	25.3	12
2.01	12.3	19
1.83	25	6.5

8. DISCUSSION AND CONCLUSIONS

The use of statistical point pattern analysis provides additional information about spatially distributed metal artifacts located within areas surveyed using the electromagnetic induction geophysical method. Data taken with the EM-63 have shown clustering of metal artifacts at the San Jacinto Battleground. The 2-dimensional K-function analysis was used to confirm that statistically significant clustering of artifacts, based on EM responses is present.

In an effort to classify and prioritize (for excavation) the clusters, the 3-dimensional Weighted K-function was employed using the channel-1 EM response mV value at first and then using the geometrically spaced time gates at which the decay signal disappears into noise. The channel-1 mV responses correlate to shallow targets. In comparison, the decay time gates indicate a better method of classification of UXO and large archaeological artifacts than the millivolt responses because of the inferred depth of burial and metallic volume of the anomaly of interest. The main drawback in using the channel-1 is that this value provides only a surface representation of the anomalies present. This means that a large response could be a large metallic object at depth or small metallic object on or very near the surface. The scale of responses in the millivolt range in these areas spanned 4-300 mV. The PPA program is sensitive to the scale size of the third dimension selected as a weighting function. Large scales of 3 magnitudes or more will produce inconclusive results because the program will be less sensitive to the lower millivolt responses of the anomalies present because of the larger spread of the weighting function values.

The time decay gates value is a more descriptive variable of the anomaly locations that pertain to buried UXO or archaeological artifacts. Objects that exhibit persistence in time will tend to be of more interest to archaeologists and geophysicists. Long time decays infer a moderate or large volume of metallic material buried at depth in the soil. This type of response differs from the channel-1 response in that if the anomaly has a significant decay time associated with it, then it is a buried object even if the millivolt reading is low. For instance, if an anomaly location has a low [mV] value (5mV) but a short decay time (2-3 time-gates) it is of a lower priority because it could be a piece of foil or a small coin near the surface that was deposited very recently.   An object with the same 5mV value but with a long decay of 15 time gates [tg] could indicate an object of moderate metallic volume buried at a depth that may be indicative of the historic time frame of the event of archaeological interest. Thus decay time gates are a more descriptive variable than the millivolt values when looking for buried objects.

In all of the 4 areas surveyed, the K-function analysis indicated clustering at small distances. Only Area A had some clustering at distance 1-2m. Statistically significant clustering at distance 1-2m was only indicated in Area 3. All other K-function clustering information is noted in the results section.

The comparison of Weighted K-function- vs -K-Function results of Area 1 conclude that Weighted K [mV] only indicated significant clustering at inter-event distance 0-1m. The confidence envelope widths *(Max L(d) – Min L(d))*are comparable at ~2m. All other clustering is secondary and will not be considered in the rest of the discussion/conclusion section. For Weighted K [tg]-vs- K-function of Area 1, There is

correlation of clustering at inter-event distance 0-1m. There is also correlation of statistically significant clustering at distances 3-4m and 4-5m. The confidence envelope is ~1.7 wide which is smaller and signifies an area of least randomness. This is better than the original Area 1K-function envelope. The correlation score is WK[mV] 1 to WK[tg] 3. WK[tg] has a narrower confidence envelope.

Comparing Weighted K-function-vs- K-function for Area 2 indicates that WK [mV] has major clustering that correlates at distance 0-1m. The confidence envelopes are~2. For WK[tg] there is major correlation also at distance 0-1. The confidence envelope is only 1.2 wide. The correlation score is WK[mV] 1 to WK[tg] 1 with a smaller confidence envelope width.

For Area 3 the Weighted K function-vs- K-function shows that WK[mV] indicates major clustering correlation at distance 0-1. There is also statistically significant clustering correlation at distance1-2. The confidence envelopes are very different with ~2.4 for K-function and ~7.5 for WK[mV]. The WK[tg] indicates no correlation of clustering at any distance. The confidence envelope is smaller at 1.6. The correlation score is WK[mV] 2 to WK[tg] 0.

The 4th area is from Area A from 2004. Weighted K-function vs K function shows the WK[mV] has no clustering correlation at any distance. The confidence envelope is very wide at ~10. For WK[tg] there is statistically significant clustering at distance 0-1. The confidence envelope is small at ~2.4. The correlation score for this area is WK[mV] 0 to WK[tg] 1.

It is concluded from this conservative analysis comparison that the Weighted K-function provides more information about the inter-event anomaly distances when using the time gates as the weighting factor. The final correlation score for this comparison was WK[mV] 4 to WK[tg] 5 keeping only major and statistically significant clustering as selection criteria.

If we look at it by area we get the same result. WK[tg] is better in Areas 1 and A while WK[mV] is better only in Area 3. Area 2 is a tie. This means that WK[tg] produces more correlation both by area and overall.

There is mention of the envelope width which favors the WK[tg] analysis. In looking closer at the data input files it appears that the confidence envelopes are influenced by the scale size of the 3rd dimensional variable. For WK[mV] with a scale of 1-300, as the scale size increases so does the confidence envelope. This is not the case for WK[tg] but the scale is only 1-26, so does not affect the envelope as much. This is why the relative envelope width was not counted in the correlation score, however, it must be mentioned that the WK[tg] envelope is always closer to the K-function envelope width.

The final area located in the Mexican Campsite used the K- function and only Weighted K-function of decay times to identify, segregate and confirm buried metallic anomalies. Weighted K using millivolt values is not the weighting scheme preferred when the targets sought are large buried metallic objects. Once confirmation of target clusters of interest is established then locating the clusters is the next step.

The final analysis of the data uses the Local Gi* Statistics analysis. While the Weighted K-function can identify clustering based on weighting functions that contain

specific information about the targets of interest, it cannot precisely locate them. The Gi* Statistic names the location of suspected important target clusters by providing the Cartesian coordinates of a cluster member. The cluster member locations can be compiled into a dig list and distributed to persons charged with excavation of the cluster members. This very important information will speed up target selection and excavation while reducing the false alarm rate.

The use archaeological formation theory was employed whenever possible for identifying the areas that were considered for geophysical EM induction surveying. Through cultural and natural formation process theory, the geophysicist is given a different outlook on ways of approaching a historical site. This knowledge aids geophysicists with their survey designs by having some a priori information supplied by archaeological theory. The end result is a more informed archaeo-geophysical study.

The data obtained from this study advances the fields of geophysical prospecting, UXO remediation and archaeology using electromagnetic data. The growing interest in preservation and documentation of historic sites has generated a new avenue for geophysicists to apply their various techniques. In this situation the archaeologist guides the geophysicist to a suspected historical area and then the geophysicist provides analysis to guide subsequent excavation procedures by the archaeologist. The combination of historic archaeological research and geophysical prospecting is becoming a more common interdisciplinary practice that yields synergistic results when conducting studies at historical sites..

Computer processing and statistical modeling skills permit the geophysicist to obtain deeper insight by improving methods of data analysis. The results of this study can be used to advocate innovative future UXO remediation and archaeological excavations. Finally the work performed here is pushing the bounds of anomaly identification and location. The work presented in this study is an initial progress towards sub-surface target prioritization for the geophysical technique of time domain EM for applications to UXO remediation and archaeological artifact recovery.

9. IMPLICATIONS FOR FUTURE RESEARCH

The new and innovative uses of Point Pattern Statistical Analysis have shown great promise in reference to this particular study. Future research would have to include the continued archaeological excavation of locations designated by the statistical analysis. The results of this study will help geophysicists with future site selection by incorporating more powerful applications of cultural and natural formation processes provided through archaeological theory. The excavations of the electromagnetic (EM) anomalies in the areas that were surveyed using the EM-63 will continue to test the hypotheses stated previously in this work.

More testing of the Weighted K-function in regards to the third (Z) variable should be performed on another site to see if using decay time gates continue to be better values than the amplitude of the millivolt [mV] response or possibly by compressing the amplitude by the square root of the value. This would also carryover to the use of the Gi* Statistics analysis since it also uses weighted data. An engineering application using the Gi* statistic technique in reverse to identify areas where roads could be built that avoid archaeological artifacts can be explored. Finally, if there were some way to streamline the analysis by creating a program that incorporates all three of the statistical programs in the proper sequence, this would surely shorten the analysis time.

REFERENCES

Aldstadt J., D-M., Chen, A. Getis, 2002, PPA: point pattern analysis (version 1.0a)*
   http://.nku.edu/~longa/cgibin/cgi-tcl-examples/generic/ppa/ppa.cgi

Butler, D.K., 2004, Report on a workshop on electromagnetic induction methods
   for UXO detection and discrimination, The Leading Edge: **23**, 776-770.

Cantrell, K., L.D. Leija, J.D. Henderson, J.F. Vasquez, K. Johnson, and S.W. Slough,
   2007, Dissolved metal abundances in bayou waters from Harris County, Texas; a
   possible monitor of subsidence in the Houston-Galveston area, Abstracts with
   Programs Geological Society of America: **39**, 58.

Cressie, N.A.C., 1993, Statistics for spatial data, Wiley, New York.

Everett, M, E., A. Benavides, C.J. Pierce, 2005, An experimental study
   of the time-domain electromagnetic response of a buried conductive plate, Geophysics:
   70, G1-G7.

Fokin, A.F., 1971, Metod pereckhodnikh protsessov pri poickakh mestorozdeniy
    sulfidnikh rud, Nedra, Leningrad USSR.

Fox, Jr., R. A., W.R. Wood, 1993, Archaeology, history, and Custer's last
   battle: The Little Big Horn reexamined: University of Oklahoma Press.
   Norman, OK.

Gabrysch, R.K., 1976, Land-surface subsidence in the Houston-Galveston Region,
   Texas, Proceedings of the Anaheim Symposium, International Association of
   Hydrological Sciences: No. 121, 16-24.

Getis, A., 1984, Interaction modeling using second-order analysis, Environ.
   Plan. A: **16**, 173-183.

Getis, A., J.K. Ord, 1992, The analysis of spatial association by use of distance
   statistics, Geographical Analysis: **24**, 189-206.

Hardin, S.L., 1994, Texan iliad: A military history of the Texas revolution, Univ
   of Texas Press: Austin TX.

Hurley, D.G., 1977. The effect of a conductive overburden on the transient
   electromagnetic response of a sphere, Geoexploration: **15**,77-85.

Johnson, M., 1999, Archaeological theory: An introduction, Blackwell Publishers Inc., Malden, MA., 149-161.

Krige, D.G., 1951, A statistical approach to some basic mine valuation problems on the Witwatersrand, J Met. Min. Chem. Soc. of South Africa: **52**, 119-139

Lee, T., 1975, Transient electromagnetic response of a sphere in a layered medium, Geophysical Prospecting: **23**, 492-512.

Lowrie, W., 1997, Fundamentals of Geophysics: Cambridge University Press UK.

Macdonald, J. A., M.J. Small, 2009, Statistical analysis of metallic anomaly patterns at former air force bombing ranges: Stoch Environ Res Risk Assess, **23**, 203-214.

Matheron, G., 1963, Principles of geostatistics, Econ Geol.: **58** 1246-1266.

McNeill, J.D., 1980, Electromagnetic terrain conductivity measurements at low induction numbers, Technical Notes, TN-6, TN-8, Geonics Ltd., Mississauga, Ontario.

Moore, S. L., 2004, Eighteen minutes: The battle of San Jacinto and the Texas independence campaign, Republic of Texas Press. TX.

Nabighian, M.N., 1984, Time domain electromagnetic methods of exploration, Geophysics: **49**, 843-1029

Nabighian, M.N., 1991, Electromagnetic methods in applied geophysics-Theory, Society of Exploration Geophysicists, Tulsa. OK.

Ord, J.K., A. Getis, 1995, Local spatial autocorrelation statistics: distribution issues and an application, Geographic Analysis, **27**, 286-306.

Parasnis, D. S., 1997, Principles of applied geophysics, Chapman & Hall, London, UK.

Parsons, S.H., 1786, Letter from Samuel Parsons to Ezra Stiles, forwarded to Thomas Jefferson, Thomas Jefferson Papers: Library of Congress

Pierce, C.J., A. Benavides, M.E. Everett, and J. Stalnaker, 2003, UXO detection improvements using EM-63 synthetic multi-receiver array geometries, SEG Technical Program Expanded Abstracts: **22**, 1227.

Rathje, W. L., M.B. Schiffer, 1982, Archaeology: Harcourt Brace Jovanovich, NY.

Renfrew, C., P. Bahn, 2000. Archaeology: Theories methods and practices: Thames & Hudson, Inc., New York.

Ripley, B.D., 1977, Modeling spatial patterns: Journal of the Royal Statistics Society B, **39**, 172-194.

Schiffer, M. B.1987, Formation processes of the archaeological record: University of Utah Press, Salt Lake City, UT.

Scott, D. D., R.J. Fox Jr., M.A. Connor, D. Harmon, 1989, Archaeological perspectives on the Battle of Little Bighorn: University of Oklahoma Press, Norman, OK.

Sharma, P. V., 1997, Environmental and engineering geophysics, Cambridge University Press, Cambridge, UK.

United States Department of Agriculture (USDA), 1976, Soil Survey of Harris County, Texas, National Cooperative Soil Survey, Washington DC.

VITA

Name: Carl James Pierce, Jr.

Address: 309-A Piez Hall
                             State University of New York at Oswego
                             Oswego, NY 13126

Email Address: carl.pierce@oswego.edu

Education: B.A., Geology, State University of New York at Potsdam,
                             2000
                             M.S., Geophysics, Texas A&M University, 2002
                             Ph.D., Geophysics, Texas A&M University, 2010